

Development of Environment Friendly New Generation MgO-C Brick Using Nano Carbon

A THESIS SUBMITTED IN PARTIAL FULFILMENT OF THE
REQUIREMENTS FOR THE DEGREE OF

Master of Technology

In

Ceramic Engineering

Submitted by

Mousom Bag



**Department Of Ceramic Engineering
National Institute of Technology
Rourkela
2011**

Development of Environment Friendly New Generation MgO-C Brick Using Nano Carbon

A THESIS SUBMITTED IN PARTIAL FULFILMENT OF THE
REQUIREMENTS FOR THE DEGREE OF

Master of Technology

In

Ceramic Engineering

Submitted by

Mousom Bag

Under the supervision of

Dr. Ritwik Sarkar

&

Dr. Sukumar Adak



**Department Of Ceramic Engineering
National Institute of Technology
Rourkela
2011**

CERTIFICATE

This is to certify that the thesis entitled, “**Development of Environment Friendly New Generation MgO-C Brick Using Nano Carbon**”, submitted by **Mr. Mousom Bag** carried out in Tata Refractories Limited, Belpahar, in partial fulfilment of the requirements for the award of Master of Technology Degree in **Ceramic Engineering** at the National Institute of Technology, Rourkela is an authentic work carried out by him under my supervision and guidance.

To the best of my knowledge, the matter embodied in the thesis has not been submitted to any other University/ Institute for the award of any degree or diploma.

I wish him all the success for his future.

Date:

Prof. Ritwik Sarkar
Dept. Ceramic Engineering
National Institute of Technology
Rourkela-769008

CONTENTS

	Page No
Abstract	i-ii
Acknowledgements	iii
List of Figures	iv-viii
List of Tables	ix-x
Chapter 1 GENERAL INTRODUCTION	1-8
1.1 Introduction	1-4
1.2 A Basic idea of MgO-C Refractory	4-5
1.3 Application of MgO-C refractory	5-8
1.4 Organization of the thesis	8
Chapter 2 LITERATURE REVIEW	9-19
2.1 Technological evolution of MgO-C refractory	9-10
2.2 Selection of raw materials	10-17
2.3 Effect of pressing methods	17
2.4 Role of ceramic nano particles in refractory industry	17-18
2.5 Role of nano carbon in low carbon MgO-C refractory	18
2.6 Objectives of the present studies	19
Chapter 3 EXPERIMENTAL WORK	20-33
3.1 Raw materials	20-22
3.2 Determination of granulometry	23-24
3.3 Fabrication of low carbon MgO-C brick	24-28
3.4 General characterization	28-
3.4.1 Surface area	28
3.4.2 Particle size distribution	28

3.4.3	Apparent porosity and Bulk density	28-33
3.4.4	Cold crushing strength	29-30
3.4.5	Hot modulus of rupture	30-31
3.4.5	Modulus of elasticity	31-32
3.4.6	Oxidation resistance	32
3.4.7	Static crucible slag corrosion test	32
3.4.8	Thermal shock resistance	33
3.4.9	Pore size distribution	33
3.4.10	Microstructure	33
Chapter 4	RESULTS AND DISCUSSION	34-67
4.1	Determination of particle size distribution by loose field density and closed packed density	34
4.2	Physical and chemical properties of nano carbon added low carbon MgO-C bricks by varying the nano carbon percentage and compared with 10% graphite containing MgO-C brick	35-42
4.2.1	Apparent porosity, Bulk density and Cold crushing strength (Before and after coking)	35-39
4.2.2	Hot modulus of rupture	39-40
4.2.3	Oxidation resistance	40-41
4.2.4	Modulus of elasticity	41
4.2.5	Summary	42
4.3	Physical and chemical properties of nano carbon added low carbon MgO-C bricks by varying the graphite percentage for a fixed nano carbon and compared with 10% graphite containing MgO-C brick	42-47

4.3.1	Apparent porosity, Bulk density and Cold crushing strength (Before and after coking)	42-45
4.3.2	Hot modulus of rupture	45-46
4.3.3	Oxidation resistance	46
4.3.4	Modulus of elasticity	47
4.3.5	Summary	47
4.4	Physical and chemical properties of nano carbon added low carbon MgO-C bricks for 5wt% graphite and 0.9wt% nano carbon by varying the anti-oxidents percentage and compared with 10% graphite containingMgO-C brick.	47-53
4.4.1	Apparent porosity, Bulk density and Cold crushing strength (Before and after coking)	48-50
4.4.2	Oxidation resistance	51
4.4.3	Hot modulus of rupture	52
4.4.4	Modulus of elasticity	53
4.4.5	Summary	53
4.5	Physical and chemical properties of nano carbon added low carbon MgO-C bricks for 3wt% graphite and0.9wt% nano carbon andvarying anti-oxidents percentage and compared with 10% graphite containingMgO-C brick.	53-59
4.5.1	Apparent porosity, Bulk density and Cold crushing strength (Before and after coking)	54-57
4.5.2	Hot modulus of rupture	57-58
4.5.3	Oxidation resistance	58

4.5.4	Modulus of elasticity	59
4.5.5	Summary	59
4.6	Some properties of nano carbon added low carbon MgO-C bricks compared with the 10% graphite containing MgO-C brick	59-67
4.6.1	Corrosion resistance	59-61
4.6.2	Thermal shock resistance	61-62
4.6.3	Microstructure	63-65
4.6.4	Pore size distribution	65-66
4.6.5	Summary	67
Chapter 5	CONCLUTIONS	68-69
	SCOPE FOR FUTURE WORK	69
	REFERENCES	70-73

Abstract:

MgO-C refractory is widely used in steel making application, mainly in steel ladles , LD converters, electric arc furnaces and also in secondary steel making. It is a basic refractory with superior slag /metal corrosion and penetration resistance and excellent thermal shock properties at high temperatures. In steel ladle applications a carbon content of 8-20 wt% is used. The function of the C is to fill the porous structure, improve the slag / metal corrosion and penetration resistance due to its non-wetting character and enhancement of thermal shock resistance due to its high thermal conductivity and low thermal expansion characteristics. Again formation of a nascent dense layer of MgO at the working surface of MgO-C brick, due to oxidation of Mg (produced on reaction between MgO and C) restricts the penetration of slag / metal components and thereby further improves the penetration and corrosion resistance. But C suffers from poor oxidation resistance and may oxidise to form CO and CO₂ resulting in a porous structure with poor strength and corrosion resistance. Prevention of carbon oxidation is done by using antioxidants, which reacts with incoming oxygen, gets oxidised and protects carbon, thus retaining the brick structure and properties. These antioxidants play a vital role in the MgO-C brick performance.

Again use of high amount of carbon in the refractory has many disadvantages too. Higher the carbon means higher thermal conductivity that results more amount of heat loss through the refractory. Again higher the heat loss, higher will be the shell temperature of the steel vessel, resulting in higher chances of deformation of shell and reduction of ladle life. Also higher carbon increases the chances of carbon pick up in steel, which is in contradiction to steel making, a decarburization process. Further, more use of carbon in refractory will increase the generation of CO and CO₂ gases and thus may become a concern for global environment. Hence, globally the researchers and scientists are considering and working for reduction in the total amount of carbon in MgO-C brick without compromising with the final characteristics. The present work is also aimed to reduce the carbon content in the MgO-C refractory brick using nano carbon, replacing the conventionally used graphite. Nano carbon content is varied from 0.3wt% to 1.5wt% and graphite was used upto 5wt%.

MgO-C bricks are prepared using conventional manufacturing technique with both pitch and resin binder. Pressing is done at 2 ton /cm² and curing is done at 200°C for 12 h. The products are

characterised in terms of bulk density, apparent porosity and cold crushing strength for both cured and coked (1000°C for 5h) conditions. Also modulus of elasticity (MOE) hot modulus of rupture (H MOR) at 1400°C, oxidation resistance at 1450°C for 5h and corrosion resistance are tested for the cured samples. All the properties are compared with conventional brick (containing 10 wt% of graphite) prepared under similar manufacturing conditions. Oxidation resistance of the nano carbon containing compositions are found to be much better than that of the conventional ones. All the batches show nearly comparable values of hot strength. 0.9wt% nano carbon containing composition is found to have optimum properties and this batch was further studied with variation in antioxidant quality and quantity. B₄C, Al are used as antioxidant and their amount is varied in the range of 0.5 -1 wt%. B₄C containing compositions are found to have improved oxidation resistance, strength and corrosion resistance.

Keywords: MgO-C refractories, Nano carbon, Low carbon MgO-C refractories.

ACKNOWLEDGEMENT

With deep regards and profound respect, I avail this opportunity to express my deep sense of gratitude and indebtedness to Prof. Ritwik Sarkar ,Department of Ceramic Engineering NIT Rourkela, for his inspiring guidance, constructive criticism and valuable suggestion throughout in this research work. It would have not been possible for me to bring out this thesis without his help and constant encouragement.

I would like to express my gratitude to Dr. Sukumar Adak,(Vice PresidentTechnology,Tata Refractories Limited, Belpahar) for allowing me to carry out my project work at Tata Refractories Limited, belpahar by his important suggestions and guidance.

I would like to express my gratitude to Prof. Sumit Pal (Faculty advisor) to his kind help and encouragement through the entire course.

I would like to express my gratitude to Prof.J.Bera, Prof. H.S. Maity, Prof. S. Bhattacharya, Prof. S.K. Pratihara, Prof. B.B. Nayak, Prof. S. Pal, Prof. D. Sarkar, Prof. R. Mazumder, Prof. A. Chowdhury for their valuable suggestions and encouragements at various stages of the work.

I would like to express my gratitude to Mr. Atanu Bal (Scientist, Tata Refractories Limited, Belpahar) for his important suggestions and guidance regarding this work.

I am also thankful to all the technology staffs of Tata Refractories Limited, Belpahar for their cooperation throughout the work.

I am also thankful to all non-teaching staffs. in Department of Ceramic Engineering for providing all joyful environments in the lab and helping me throughout this project.

I am also thankful to research scholars in Department of Ceramic Engineering for providing all joyful environments in the lab and helping me throughout this project.

I want to express thank to my friend Mr. Tapas Mahata for his continuous support.

Last but not least, my sincere thanks to all my family members and friends who have patiently extended all sorts of help for accomplishing this undertaking.

Date:

Mousom Bag

List of Figures:	Page No.
Fig.1.1: Ladle lining with different refractories.	7
Fig.2.1: Crystal structure of MgO.	11
Fig.2.2: Crystal structure of graphite.	12
Fig.3.1: BET surface area graph of graphite.	21
Fig.3.2: BET surface area graph of nano carbon black.	22
Fig.3.3: Particle size distribution of nano carbon black.	22
Fig.3.4: Flow chart of determination of granulometry.	23
Fig.3.5: Schematic diagram for CCS	30
Fig.3.6: HMOR machine	31
Fig.4.1: Variation of apparent porosity with the variation of nano carbon content.	35
Fig.4.2: Variation of bulk density with the variation of nano carbon content.	36
Fig.4.3: Variation of cold crushing strength with the variation of nano carbon content.	37
Fig.4.4: Variation of coked apparent porosity with the variation of nano carbon content.	38
Fig.4.5: Variation of coked bulk density with the variation of nano carbon content.	39
Fig.4.6: Variation of coked cold crushing strength with the variation	

	of nano carbon content.	39
Fig.4.7:	Variation of hot modulus of rupture with the variation of nano carbon content.	39
Fig.4.8:	Variation of oxidation resistance with the variation of nano carbon content.	40
Fig.4.9:	Variation of modulus of elasticity with the variation of nano carbon percentage.	41
Fig.4.10:	Variation of apparent porosity with the increase of graphite content.	42
Fig.4.11:	Variation of bulk density with the increase of graphite content.	43
Fig.4.12:	Variation of cold crushing strength with the increase of graphite content.	43
Fig.4.13:	Variation of coked apparent porosity crushing strength with the increase of graphite content.	44
Fig.4.14:	Variation of coked bulk density with the increase of graphite content.	44
Fig.4.15:	Variation of coked cold crushing strength with the increase of graphite content.	45
Fig.4.16:	Variation of hot modulus of rupture with the increase of graphite content.	45
Fig.4.17:	Variation of oxidation resistance with the increase of graphite	

	content.	46
Fig.4.18:	Variation of modulus of elasticity with the variation of nano carbon percentage.	47
Fig.4.19:	Change in apparent porosity with the variation of antioxidants.	48
Fig.4.20:	Change in bulk density with the variation of antioxidants.	48
Fig.4.21:	Change in cold crushing strength with the variation of antioxidants.	49
Fig.4.22:	Change in coked apparent porosity with the variation of antioxidants.	49
Fig.4.23:	Change in coked bulk density with the variation of antioxidants.	50
Fig.4.24:	Change in coked cold crushing strength with the variation of antioxidants.	50
Fig.4.25:	Change in oxidation resistance with the variation of antioxidants.	51
Fig.4.26:	Oxidation samples after cutting.	51
Fig.4.27:	Change in hot modulus of rupture with the variation of antioxidants.	52
Fig.4.28:	Variation of modulus of elasticity with the variation of anti-oxidants.	53
Fig.4.29:	Change in apparent porosity with the variation of antioxidants for 3 wt% graphite.	54
Fig.4.30:	Change in bulk density with the variation of antioxidants with 3 wt% graphite.	54
Fig.4.31:	Change in cold crushing strength with the variation of anti-oxidants with 3 wt% graphite.	55
Fig.4.32:	Change in coked apparent porosity with the variation of	

	anti-oxidants with 3 wt% graphite.	56
Fig.4.33:	Change in coked bulk density with the variation of antioxidants with 3 wt% graphite.	56
Fig.4.34:	Change in coked cold crushing strength with the variation of anti-oxidants with 3 wt% graphite.	57
Fig.4.35:	Change in hot modulus of rupture with the variation of anti-oxidants with 3 wt% graphite.	57
Fig.4.36:	Change in oxidation resistance with the variation of antioxidants with 3 wt% graphite.	58
Fig.4.37:	Variation of modulus of elasticity with the variation of anti-oxidants.	59
Fig.4.38:	Corroded samples after cutting.	60
Fig.4.39:	Graph of penetration depth of Static corrosion test.	61
Fig.4.40:	Graph of thermal shock resistance.	62
Fig.4.41:	Samples after 4 th cycle.	62
Fig.4.42:	Samples after 10 th cycle.	62
Fig.4.43:	(a) SEM picture of 3 wt% graphite and 0.3% nano carbon containing low carbon MgO-C brick (b) It's carbon mapping.	63
Fig.4.44:	(a) SEM picture of 3wt% graphite and 0.9 wt% nano carbon containing low carbon MgO-C (b)It's carbon mapping.	63
Fig.4.45:	(a) SEM picture of 3wt% graphite and 0.9 wt% nano carbon containing low carbon MgO-C (b)It's carbon mapping.	64

Fig.4.46:	(a) SEM picture of 10 wt% graphite containing MgO-C brick.	
	(b) It's mapping.	64
Fig.4.47:	Incremental intrusion Vs pore size of sample with 3wt% graphite 0.3% nano carbon.	65
Fig.4.48:	Incremental intrusion Vs pore size of sample with 3wt% graphite 0.6% nano carbon.	65
Fig.4.49:	Incremental intrusion Vs pore size of sample with 3wt% graphite 0.9% nano carbon.	66
Fig.4.50:	Incremental intrusion Vs pore size of sample with 10% graphite.	66

List of Tables:	Page No:
Table.1.1: Different MgO-C refractory in different zone of BOF.	5
Table.1.2: Different working lining designs in steel ladles in India.	7
Table.2.1: Technological development of MgO-C refractory brick.	9-10
Table.2.2: Chemical and physical properties of magnesia aggregate.	12
Table.2.3: Characteristics of flake graphite used for carbon containing refractories.	13
Table.3.1: Chemical composition in percentage of fused magnesia.	20
Table.3.2: Physical and chemical analysis of flake graphite.	20
Table.3.3: Physical and chemical analysis of pitch powder.	21
Table.3.4: Physical and chemical analysis of liquid resin.	21
Table.3.5: Physical and chemical analysis of nano carbon black.	21
Table3.6: Batch composition of MgO-C varying nano carbon for a particular percentage of graphite.	24
Table3.7: Batch composition of MgO-C varying graphite content for a particular percentage of nano carbon.	25
Table.3.8: Batch composition of MgO-C varying anti -oxidant content for a 0.9wt% of nano carbon and 5wt% of graphite.	25
Table.3.9: Batch composition of MgO-C varying anti -oxidant content	

	for 0.9wt% of nano carbon and 3wt% of graphite.	26
Table.3.10:	Mixing sequence of MgO-C bricks.	26
Table.3.11:	Chemical composition(wt%) and basicity of the steel making ladle slag.	32
Table.4.1:	Determination of granulometry.	34

Chapter-1
GENERAL INTRODUCTION

1.1 Introduction:

Technological improvement in the manufacturing of iron and steel has changed significantly the operating practice. Increase in furnace capacity, operating temperature, hot-metal temperature and throughput are common to all units. These radical changes along with the need of improved practices for better manufacturing and application environment are demanding a new generation of refractory material with improved properties, performance and life with eco-friendliness.

Refractory, a non metallic inorganic material, with very high melting temperature, excellent mechanical properties both at room temperature and at high temperatures and high resistance to withstand rapid temperature fluctuations, including repeated heating and cooling. They have also good corrosion and erosion resistance to molten metal, glass, slag and hot gases etc. Because of good thermal stability of refractories they are used in kilns, furnaces, boilers, incinerators and other applications in industries like iron and steel, non ferrous metal, cement, glass, ceramics, chemicals etc.

Many of the scientific and technological inventions and developments would not have been possible without refractory materials. Manufacturing of any metal without the use of refractory is almost impossible. The ASTM C71 defines the refractories as “nonmetallic materials having those chemical and physical properties that make them applicable for structures or as components of systems that are exposed to environments above 1000 °F (538 °C)” [1]. The type of the refractory to be used is dictated by the conditions prevailing in the application area. Generally refractories are classified into two different groups [2]:(a) based on raw materials , the refractories are subdivided into three categories such as acidic (Zircon, fireclay and silica), basic (dolomite, Magnesite, magnesia-carbon, alumina-magnesia – carbon, chrome-Magnesite and Magnesite- chrome) and neutral (alumina, chromites, Silicon carbide , carbon and mullite) and (b) based on manufacturing process , the refractories are subdivided into two categories such as shaped refractories (available in the form of different brick shapes ,and includes the oxide and non-oxide systems) and unshaped refractories which includes mortars, castables and other monolithics).

Refractories of iron & steel industries encounter a very stringent environment. There is a heavy load of molten metal at very high temperature (>1600°C), corrosive slag attack, FeO corrosion from metal, abrasion and thermal/mechanical spalling caused by molten metal and slag, etc. Again there is always a challenge from further improvement in the metal extraction technology up-gradation, higher temperature of operation, longer service life.

Hence use of advanced refractory lining with very high corrosion and spalling resistance, excellent mechanical characteristics even at high temperature with ease of application and enhanced lining life, less down time and environmental friendliness are essentially required. Being a major consumer of refractory, iron and steel industries control the demand and supply market of the refractory. As the production of crude steel is increasing with time, the production of refractory has also increased significantly. Besides, there has been a drastic change in the refractory technology in recent years. Strong demands are emphasized in various fields; like extended service life of the steel ladles, rationalization, improvement of working environment, energy saving and production of material with higher quality etc. Presently the expected crude steel production in the current fiscal of India is expected to be ~ 70 Million tons. The steel sector in India is growing very fast and expert are expecting a production ~ 100-120 million tons by 2020[3]. Maintaining the pace of the steel sectors, refractory industries are also growing very rapidly.

In tune with the changing trends in steelmaking, especially in ladle metallurgy, the high performing shaped refractories are on an increasing demand in recent years. The higher campaign lives and the variability of the newer steel making operations are decided by the availability and performance of such shaped refractories with superior high temperature mechanical strength, erosion and corrosion resistance [4]. Initially the ladles were used only to transport the steel from steel making unit to casting bay, but now a day the refining process is also carried out in the same. Thus steel producers through the world have been putting on a continuous effort to improve the ladle life in order to increase the performance of ladles as well as reduce the specific consumption of refractories so as to have a strong grip over cost and quality of steel and also to increase the ladle availability with lesser number of ladles relining per day [5]. Due to the above reasons, there had been a great technological evolution in ladle lining concept such as: Zonal lining concept, which deals with both selection of refractory quality and refractory lining thickness [6-9].

MgO-C bricks have dominated the slag line of ladles for at least a decade as they possess superior slag penetration resistance and excellent thermal shock resistance at elevated temperature because of the non- wetting properties of carbon(graphite) with slag, high thermal conductivity, low thermal expansion and high toughness [10,11]. Increased steel production has lead both refractory manufacturers and users to resume interest on further improvement of thermo-chemical properties of MgO-C refractories [12]. Presence of nano (size<100 nm) particles in MgO-C refractories has also improved the durability, thermal shock resistance, corrosion resistance and oxidation resistance [13-15].

Again formation of a nascent dense layer of MgO at the working surface of MgO-C brick, due to oxidation of Mg (produced on reaction between MgO and C) restricts the penetration of slag / metal components and thereby further improves the penetration and corrosion resistance. But C suffers from poor oxidation resistance and may oxidize to form CO and CO₂ resulting in a porous structure with poor strength and corrosion resistance. Prevention of carbon oxidation is done by using antioxidants, which reacts with incoming oxygen, gets oxidized and protects carbon, thus retaining the brick structure and properties. These antioxidants play a vital role in the MgO-C brick performance.

Again use of high amount of carbon in the refractory has many disadvantages too. Higher the carbon means higher thermal conductivity that results more amount of heat loss through the refractory. Again higher the heat loss, higher will be the shell temperature of the steel vessel, resulting in higher chances of deformation of shell and reduction of ladle life. Also higher carbon increases the chances of carbon pick up in steel, which is in contradiction to steel making, a decarburization process. Furthermore, use of carbon in refractory will increase the generation of CO and CO₂ gases and thus may become a concern for global environment. Hence, globally the researchers and scientists are considering and working for reduction in the total amount of carbon in MgO-C brick without compromising with the final characteristics. The lining of ladle depends to a greater extent on the wear rate of MgO-C refractory arising from slag penetration and structural spalling. With the development of secondary refine techniques of steel the production rate of high purified steel has increased dramatically. So it is aimed globally to reduce the carbon content in MgO-C refractory.

Use of nano carbon, having high surface area resulting in a wide distribution of carbon particles even at low percentages, the entire matrix of the brick can be covered [16]. Again the fixed carbon which comes from the graphite and resin in conventional brick has glassy phase in nature but by introducing nano carbon the fixed carbon has graphite phase. Being graphite phase it's mechanical strength as well as oxidation resistance is better than glassy phase. By introducing nano carbon in the MgO-C refractory the pore size could be further minimized and therefore it is possible to achieve improvement in corrosion resistance. Nano particles are dispersed in the resin, and during the curing time large number of micro cracks are developed due to shrinkage from evaporation of volatile materials. strength further[17-20]. In the existing MgO-C Refractories, high thermal conducting graphite promotes the diffusion of the thermal shock profile generated in the refractory body and result in an excellent ability to absorb the mechanical stress due to the thermal expansion and shrinkage, On the other hand, in new technology it was found that flexibility of the nano

particle boundaries in the nano structured matrix and nanometer size porosity generated during the dissipation of volatile matter in the resin component by control of the carbonization process, absorbed the thermal expansion and shrinkage generated in the individual refractory particles.

1.2 A Basic idea of MgO-C Refractory:

MgO-C brick is a composite material based on MgO and C and bonded by high carbon containing pitch and resin, with some metallic powder as anti-oxidants to protect the carbon. These MgO-C bricks are made by high pressure and are of unburned type. These are known to possess excellent resistance to thermal shock and slag corrosion at elevated temperatures. Thus these materials have found extensive applications in steel making processes especially in basic oxygen furnaces, electric arc furnaces, lining of steel ladles, etc [21].

MgO-C bricks have the following features:

1. High refractoriness as no low melting eutectic occurs between MgO and C.
2. Graphite, the carbon source, has very low thermal expansion; hence in the composite form of MgO-C the thermal expansion is low.
3. Graphite, having a unshared free electron, has very high thermal conductivity, which imparts high thermal conductivity in the MgO-C composite,
4. As the thermal expansion is low and the thermal conductivity is high the thermal shock resistance of MgO-C is very high.
5. Non wettability of carbon gives similar character to MgO-C bricks and thus it prevents the penetration of slag and molten steel.
6. Better ability to absorb stress, thus keeping down the amount of discontinuous wear due to cracks.

Main constituents of MgO-C bricks:

1. Magnesia grains are the main constituent of the system and offer very high resistance to basic slag corrosion, but suffer from poor thermal shock resistance.
2. Graphite imparts non-wetting nature to MgO-C that improves the corrosion and improves thermal shock resistance of the system but it is susceptible to oxidation.
3. Antioxidants that tend to retard overall kinetics of oxidation of carbon and improve high temperature strength by the formation of carbides.

4. Binder that keeps the different components of the refractory together. Volatiles from the binder are the first to go out leaving behind carbon.

1.3 Application of MgO-C brick:

Converters:

After the development the MgO-C brick was applied in basic oxygen furnaces. Now a day the entire lining is done by MgO-C brick. These bricks have enhanced the productivity of steel making by increasing the furnace availability. By using MgO-C bricks clean steel can be produced with less refractory consumption [22].

Table.1.1: Different MgO-C refractory in different zone of BOF.

Application area	Refractories used
Top conical	Normal MgO-C brick
Tap hole sleeves,	MgO-C
Barrel	More fused magnesia (large crystal) less SWM, carbon content 12-13 %
Bottom conical	Less carbon content 8-10 wt%, more SWM
Bottom	Combination of Sea water magnesia and fused magnesia with carbon containing 8 wt%.

However, improved operating conditions and repair technologies have significantly extended the service life of the converter linings and hence the amount of MgO-C bricks used for converter linings should decrease in future.

Electric furnaces:

Since the development of Electric furnaces in 1970's the MgO-C bricks are applied in most of its lining areas. Now they are used mainly in hot spots and furnace bottoms, including the

slag line. Now a day they have also been used for bottom blowing plugs, the sleeves of furnace-bottom tap holes and furnace bottom electrodes of DC electric furnaces [23].

Secondary refining furnaces:

The use of MgO-C bricks has been considered for reduced pressure operations, for example, in RH degasser where the MgO-C reaction has seemed to be a source of trouble. This reaction is more significant at lower pressure at high temperatures. However, the effect of a slag coating on bricks may eliminate the problems at hot surface. Therefore MgO-C bricks may be usable in furnaces operating under reduced pressure [21].

Ladles:

Refractories used for ladle lining must able to withstand the increasing severity of service conditions associated with the secondary steel making in order to produce various grades of steel with stringent specifications. The condition during the steel refining processes are aggressive, which makes the refractory materials used in steel teeming ladles susceptible to high degree of corrosion. In addition to corrosion, brittle nature of refractory materials gives limitation to their applicability [24-26].

Some of the important properties requirements of refractories used in steel ladle are:

- ❖ High corrosion resistance to steel and slag
- ❖ High abrasion resistance by liquid metal
- ❖ High thermal spalling resistance
- ❖ High hot strength and
- ❖ Low molten steel penetration

Fig.1.1: shows the schematic view and various zones of steel ladle. The different working lining designs of the steel ladle is given in table 1.2.

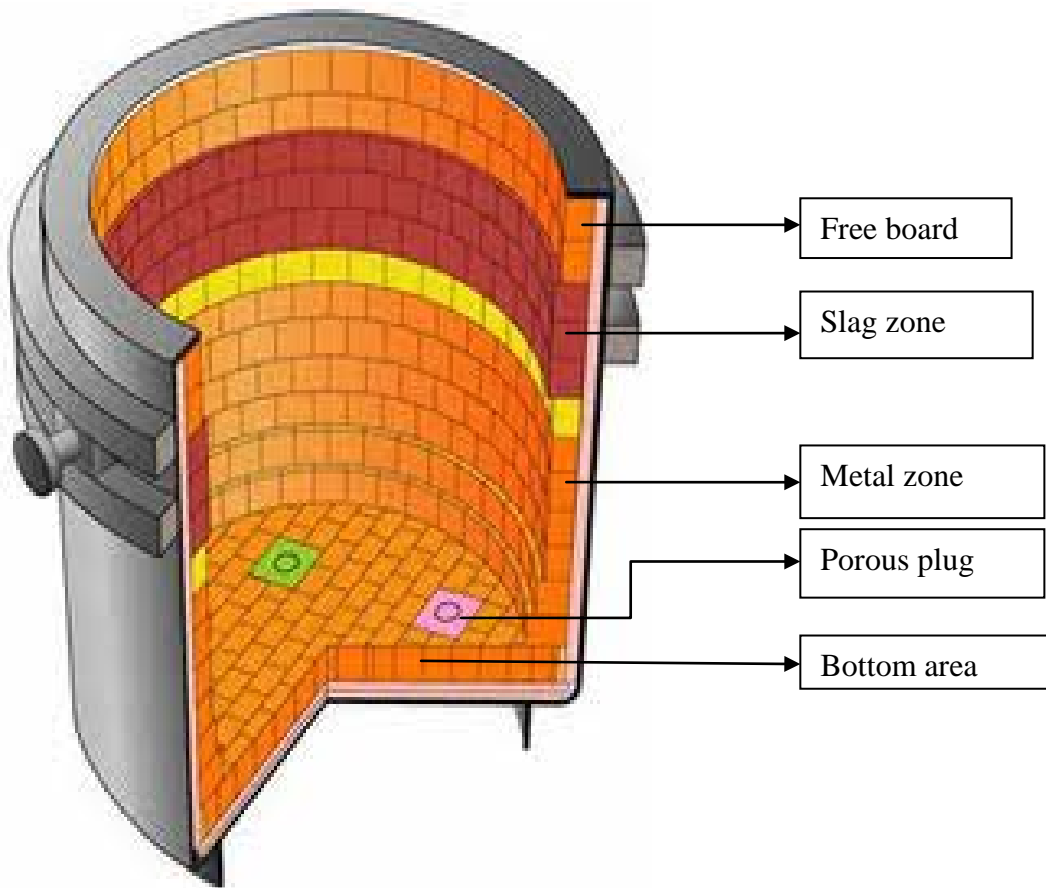


Fig.1.1: Ladle lining with different refractories.

Table1.2: Different working lining designs in steel ladles in India

Area	Bottom	Metal Zone	Slag Zone	Free Board
Refractory bricks used	MgO-C	MgO-C	MgO-C	MgO-C
	Al ₂ O ₃ - MgO-C	Dolomite	70% Al ₂ O ₃	70% Al ₂ O ₃
	70% Al ₂ O ₃	Al ₂ O ₃ - MgO-C	80% Al ₂ O ₃	80% Al ₂ O ₃
	80% Al ₂ O ₃	70% Al ₂ O ₃	MgO-Cr ₂ O ₃	Cr ₂ O ₃ - MgO
	MgO-Cr ₂ O ₃ 80% Al ₂ O ₃)	80% Al ₂ O ₃ Cr ₂ O ₃ - MgO		

For the past several years, refractories based on MgO and C had performed tremendously well in many applications such as basic oxygen furnace (BOF), electric arc furnace (EAF), varieties of vessels and ladles for secondary refining treatments as compared to bricks without carbon due to high thermal conductivity, low thermal expansion, non-wetting nature

and chemical inertness to slag and high thermal shock resistance of carbon present in the system.

MgO-C refractory, one of the highest consumable refractory item in steel sector with a specific consumption as high as 3.0 kg/ton in BOF and 2.5 kg/ton in EAF for the best shop's practice, is the top most concern for any steel manufacturer. MgO-C refractories are unfired refractory, which is manufactured by mixing magnesia aggregates & fines, graphite and other additives with liquid resin and pitch as a binder. Next the mix is uni-axially pressed using hydraulic press with a specific pressure of 2 T/cm². The pressed bricks were then tempered at 200 – 400° C for about 12 h to facilitate the polymerization of resin into carbon and to eliminate residual water, volatile matters and phenols, thereby developing sufficient strength. The physical, thermal, thermo-mechanical and thermo –chemical properties of MgO-C refractories have improved significantly by selecting the right raw materials with respect to purity, grain size of MgO, binders, bonding systems and additives in nano range [26-29].

1.4 Organization of the thesis:

The addition of nano particles has a great effect on the properties of refractories due to it's smaller particle size and larger surface area. Carbon is added in the MgO-C bricks for improving the thermal spalling and slag, metal penetration resistance due to higher conducting value and low wetting properties of carbon respectively. The addition of nano carbon in MgO-C brick has largely improved the mechanical and thermo-mechanical properties of MgO-C refractories and which is discussed. The basic idea of MgO-C brick has been discussed in chapter 1. Chapter 2 consists of the application of MgO-C refractory, literature regarding the various works on MgO-C refractories, the required properties of different ingredients of MgO-C brick and the role of nano particles and nano carbon for the development of different refractories. The main aim of the work has been discussed at the end of chapter 2. Chapter 3 explains about different raw materials used and different methods followed for the present work. It also covers the different characterization techniques of MgO-C refractory brick. The results of the experimental work are fully described in chapter- 4. It explains the different physical and chemical properties of low carbon MgO-C brick. The comparison of nano carbon added low carbon MgO-C brick with the conventional i.e. 10% graphite content MgO-C brick is done. Finally the conclusion and scope for the future work is discussed in chapter-5.

Chapter 2:
LITERATURE REVIEW

2. Literature review:

2.1 Technological evolution of MgO-C refractory:

After 1950's, carbon has been recognized as a very important component of refractories. It has been found that by addition of carbon results to a better thermal and chemical resistance and hence the life of refractory linings has been increased and indirectly reduces steel production cost[30,31]. Now a days carbon is an very essential component of the ceramic –carbon composite for many refractory applications . State-of- the art, magnesia–carbon brick is taken as standard for lining of ladle metallurgy furnaces for slag lines, basic oxygen furnaces and electric arc furnaces for steelmaking and also in secondary steel making vessels[32]. The details of technological development of MgO-C refractories with its application areas are given in Table 2.1.

Table.2.1: Technological development of MgO-C refractory brick [33, 34].

Year	Technological Evaluation
1950	❖ Evolution of pitch bonded dolomite refractories and magnesia carbon brick and their application; Carbonization was done during the preheating treatment of ladle; better thermal –spalling resistance, inhibiting the slag penetration.
	❖ Application area is Basic Oxygen Furnaces.
1970	❖ Magnesia purity became a under a consideration .Thus Magnesia grain with lime to silica ratio of 2 to 3: 1 and low boron content was used extensively to increase the life of brick by improving the corrosion resistance.
	❖ Burned and impregnated magnesia brick was developed with fine pore size to inhibit slag penetration thus improve corrosion resistance and thermal spalling.
	❖ Applied in charge pad and other high wear and impact areas in Basic Oxygen Furnaces.
	❖ Zonal lining concept was started.
	❖ Resin bonded magnesia-graphite refractories were developed with higher carbon content.

1980

- ❖ To preserve the carbon and make the brick strengthen antioxidants were used.

-
- ❖ To further improve the corrosion resistance high purity magnesia grains (fused/ sintered) having large crystal size is used.
 - ❖ The type and amount of carbon content is varied to improve the thermal conductivity and oxidation resistance.
 - ❖ Various additives (such as metallic, alloy and inorganic compounds) is added to achieve better hot strength, oxidation resistance and corrosion resistance.

2000-

Till date

- ❖ To improve thermal spalling and corrosion resistance in-situ spinel bonding is done.
 - ❖ Various nano additives are added.
 - ❖ Reduction of carbon content.
-

Though several efforts have been taken to improve the performance of MgO-C bricks, the problems are still there due to increasing severity of operating condition by many folds. This has created enormous opportunities for further research in this field.

The selection of base raw materials has great influences on the properties and performance of refractories and was discussed in detail.

2.2 Selection of raw materials:

The main problems faced in steel ladle refractories are oxidation of carbon layer, heat loss of steel due to the high conductivity of carbon, deterioration of strength at high temperature, corrosion by steel slags, thermal spalling, abrasion by liquid metal, and molten steel penetration [35-37]. The raw materials play a great role on the performance and life of the refractories. Several research works had been carried out to find out the effect of different raw materials based on purity, porosity and crystallite size [38-40]. The main raw materials

are magnesia, graphite, binder like pitch powder and resin, and various metal powders as antioxidants. Details of the each of the raw materials are described below.

(1) Magnesia

For the production of MgO-C bricks magnesia is the major raw material containing about 80 wt% or more of the total batch. Three different types of magnesia grains are used such as – fused magnesia produced by fusing magnesia in an electric furnace, seawater magnesia produced by very high temperature firing of magnesium hydroxide extracted from seawater and sintered magnesia produced from natural magnesite[41-42].

Several works had been done to study the effect of magnesia aggregate on the corrosion and abrasion resistance of MgO-C bricks. It was reported that for superior corrosion and abrasion resistance of the final MgO-C brick the magnesia aggregate should have the following characteristics.

- (i) Large periclase crystal grain to reduce the extent of grain boundary [43].
- (ii) High concentration of fused magnesia than that of sintered magnesia [40, 44].
- (iii) High ratio of CaO/SiO_2 and small content of B_2O_3 [43,45-46].
- (iv) High purity and minimum impurity of magnesia.

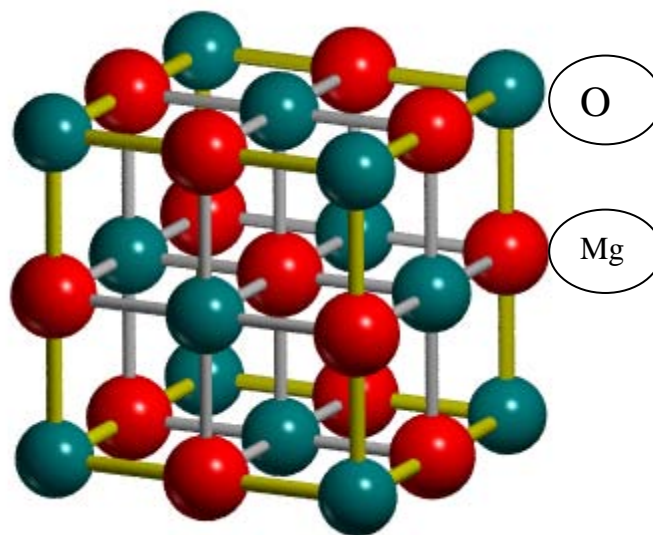


Fig.2.1: Crystal structure of MgO.

The typical chemical and physical properties of magnesia aggregate are given in table 2.2.

Table.2.2: Chemical and physical properties of magnesia aggregate [43, 45].

		Products					
Properties		Seawater		Natural		Brine	
		Fused	Sintered	Fused	Sintered	Fused	Sintered
Chemical	MgO	99.02	99.14	96.56	98.22	95.56	99.38
Composition	SiO ₂	0.22	0.23	1.29	0.57	1.96	0.02
(%)	Al ₂ O ₃	0.06	0.06	0.12	0.08	0.90	0.05
	Fe ₂ O ₃	0.11	0.04	0.75	0.44	0.67	0.01
	CaO	0.57	0.51	1.19	0.58	0.98	0.67
	B ₂ O ₃	0.02	0.04	Traces	Traces	Traces	Traces
A. P. (%)		2.60	1.50	1.10	0.80	8.0	2.0
B. D. (gm/cc)		3.46	3.40	3.54	3.55	3.20	3.43
Grain size (μm)		>200	20-40	>50	>100	20-60	20-40

A.P. = Apparent porosity, B. D. = Bulk density

(2)Graphite:

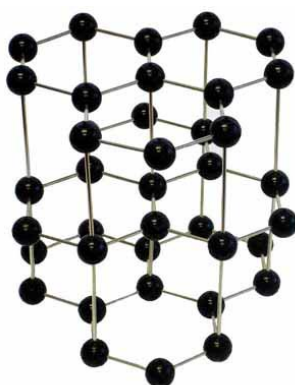


Fig.2.2: Crystal structure of graphite.

In MgO-C brick, carbon plays very vital role by providing non-wetting nature to the refractory. Now the carbon source used is graphite. Among different commercial sources of carbon, graphite shows the highest oxidation resistance. Carbon, when used in oxidizing atmosphere. Like in

furnaces as refractories, gets oxidized, resulting a porous structure with very poor strength. Hence resistance against oxidation is very important for the carbon source. Again due to the flaky nature it imparts higher thermal conductivity and lower thermal expansion, resulting in very high thermal shock resistance. Hence the carbon source used is flaky graphite, which is available in nature as well formed crystals by increasing the graphite content the compressibility increases during pressing and results in a decrease in the porosity. However, due to the irreversible expansion of graphite at higher temperatures, this effect was diminished. Calculation of the oxidized layer thickness changes with oxidation time, based on the weight loss results of TG test and the proposed equations showed that with increase in graphite content, the thickness of oxidized layer decreased even if the weight loss increased. These results were successfully explained by determining changes of the effective diffusion coefficient as well as the graphite molar density with the changes of graphite content.

Characteristics of flake graphite are given in table 2.3.

Table2.3: Characteristics of flake graphite used for carbon containing refractories [47-48].

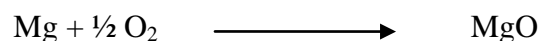
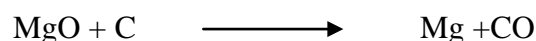
Characteristics	Source				
	China	India	Malaysia	Japan	
	1	2			
: Grain size distribution (wt %)					
>0.5 mm	13.2	0.9	2.6	12.5	-
0.50- 0.297 mm	35.0	8.8	28.2	27.4	-
0.297- 0.177 mm	26.3	49.2	65.6	40.4	6.8
0.177- 0.125 mm	11.4	38.4	2.9	13.3	12.6
0.125- 0.063 mm	8.9	2.3	0.5	5.1	42.6
< 0.063 mm	5.1	0.3	0.3	1.1	38.0
Avg. Grain size (mm)	0.287	0.195	0.261	0.275	0.074
Ash content (%)	14.4	5.9	12.7	11.9	13.4
Minerals in ash:					
Quartz	#	#	###	#	##
Mica (Biotite)	#	#	##	###	-
Kaolinite	##	#	##	#	-
Chlorite	#	-	-	-	#
Feldsper	-	#	#	-	#
Vermiculite	#	#	#	##	#

###very strong, ## strong , # Weak , - Very weak

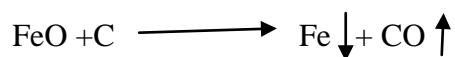
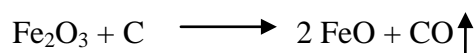
Presence of some minerals has adverse effect on the corrosion resistance of MgO-C brick. Such as quartz, kaolinite and anorthite in ash of graphite decreases the corrosion resistance of MgO- C brick. After decomposition the impurities of flake graphite reacts with MgO grains and forms low melting phases. Thus decreases the corrosion resistance [49]. Hence, the ash content of graphite should be as low as possible and purity should be very high.

The roles of graphite are

- (i) Graphite covers the spaces of magnesia grains and fills porous brick structure,
- (ii) The contact angle of graphite is very high. So it prevents the slag penetration in to the brick due to high wetting angle between slag and graphite.
- (iii) At higher temperature magnesia is reduced to pure magnesium by carbon and this vaporized magnesium comes to the surface of the brick and again oxidized to magnesia. The formation of a dense layer of MgO and CO at the slag- brick interface prevents further penetration of oxygen into the brick.



- (iv) Due to high thermal conductivity and low thermal expansion of graphite, improves the thermo – mechanical properties and spalling resistance of the brick. The size of graphite has a great role for improving the abrasion, corrosion and oxidation resistance of MgO- C bricks [50].
- (v) Slag containing Fe_2O_3 has higher corrosive action than that of containing FeO. Carbon reduces Fe_2O_3 to FeO and further reduction of FeO produces metallic iron, enriches the production of steel.



Graphite has the tendency of compressibility in the mixture to get a dense structure .This is the major problem faced during the manufacturing of MgO-C brick. Also the binder has a great role on the pressing of a dense brick.

(3) Resin:

Initially, pitch was used as binder for MgO-C brick. When pitch or tar bonded carbon refractories are cured by producer or burned by the user to be put into service, large amount of fumes are liberated. These fumes are very toxic because of their high content of Polycyclic aromatic compounds (PAC) such as benzo α pyrenes.(BAP) in the case of pitch or tar mixes or phenols or cresols in the case of phenolic resin [51]. However, due to the elastic character of graphite, it was very difficult to prepare a dense MgO- C brick containing a larger amount of flake graphite. It causes the brick to expand during heat treatment and leads to poor adhesion of graphite to the matrix. Also by using pitch it was necessary to hot pressing of the mixture. So resin was found to be the best binder for MgO-C refractories.

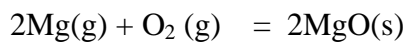
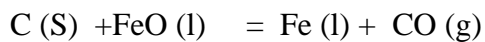
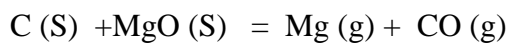
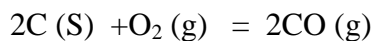
Phenolic resin is the most effective binder used in carbon containing refractories. It has the following excellent features:

- (i) It has high content of fixed carbon, resulting in a strong bonding in the system.
- (ii) High handling strength due to its strong bonding property.
- (iii) It possesses high dry strength because it is thermosetting in nature.
- (iv) It has high chemical affinity towards graphite and refractory aggregates.
- (v) It is less harmful than tar or pitch so it is more environment friendly.
- (vi) It has very excellent kneading and pressing characteristics.
- (vii) Polymerization of resin occurs due to tempering at ($\sim 200^{\circ}\text{C}$) and leads to isotropic interlocking structure.
- (viii) The cold crushing strength (CCS) increases with the increase of resin content.

The desired viscosity of resin to be used for MgO-C brick is 8000 cps at 25°C . The viscosity of resol resin increases sharply with decrease in temperature, so very often in winter it causes low dispersion of ingredients in the mixer machine [52]. On the other hand, in summer, the viscosity of resin decreases. Sometimes it causes the green body to weaken its stiffness and resulting in lamination of bricks. In order to overcome the reduction in viscosity, the powder novalac resin was added along with the liquid resol resin [52]. Increase in resin content improved compressibility during pressing and consequently increased the CCS of the tempered samples. The TGA analysis at 1000°C showed that the mass loss of the system containing phenolic resin is a little bigger than those of the systems containing the polymeric resins with the attached different metals [51]. Among various resin types, the resol type resin is best as binder. Because of its lower viscosity and lower content of volatile species the samples containing resol had the lowest porosity after heating at high temperature.

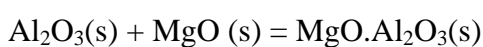
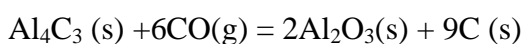
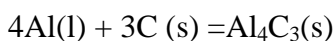
(4) Antioxidants:

Oxidation of carbon was one of the main drawbacks of carbon containing refractories. The oxidations of carbon in MgO-C refractories happen in two ways (a) direct oxidation and (b) indirect oxidation. Direct oxidation occurs below 1400 °C and carbon is oxidized directly by the oxygen from atmosphere. Indirect oxidation occurs above 1400 °C where carbon is oxidized by the oxygen from MgO or slag. The resulting Mg gas reaction oxidizes again and generates MgO which is called the secondary oxide phase or the dense layer. It is claimed that the secondary oxide phase protects the brick against oxidation by preventing oxygen ingress [53-56]

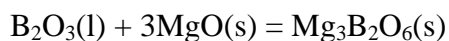
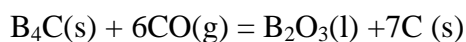


Due to exposure to temperature above 1500°C, Magnesium vapor forms and simultaneously deoxidizes to MgO. A dense secondary phase of Magnesia layer adjacent to the hot face of the refractories was formed, results an increase in oxidation resistance of the material during operation at high temperature. Thus to prevent oxidation of carbon, different antioxidants such as Magnesium (Mg), aluminum (Al), Silicon (Si), Boron Carbide (B₄C) are used in MgO- C refractories. Due to the low cost and high effective protection Al and Si antioxidants are mostly used, which after formation remain stable as a discrete phase in the bulk of the specimen.

In service, carbon interacting with the aluminium forms Al₄C₃ greater than 750°C then greater than 1100°C Al₄C₃ forms Al₂O₃. Finally greater than 1400°C it forms MgO.Al₂O₃ spinel [57]. Spinel formations results in volume expansion, apparent porosity reduction and fill the pores. Thus helps in further oxidation and improves corrosion resistance.



B₄C perform much better oxidation resistance than Al. B₄C reacts with the CO forms B₂O₃. The form B₂O₃ on reaction with MgO transforms to a liquid phase compound MgO.B₂O₃ [58].



Thus B_4C protects the carbon of MgO-C bricks and improves the life.

2.3 Effect of pressing methods:

Yakafumi Harada et.al [59] studied that the characteristics of the MgO-C brick have an orientation dependence caused by the orienting property of graphite. They compared the characteristics of the samples formed in a friction press (FP) and cold isostatic press (CIP) with the changes in graphite content and grain size. They concluded that an orientation dependent of the thermo-mechanical properties was confirmed even in the CIP body, although the degree of orientation dependence was less than that in the FP body. The higher the graphite content, the higher the orientation dependence of the thermo-mechanical properties. The larger the grain sizes of the graphite, the higher the orientation dependence of the thermo-mechanical properties [60].

2.4 Role of ceramic nano particles in refractory industry:

The refractory industry is enough matured and in order to counteract the stiff competition from global market, the one of the best way to develop new technologies that have high added value and also it cannot be copied easily. Thus the application of nano particles has brought about a tremendous change in refractories field by exhibiting remarkable performance [13-15]. Nano particles are nothing but ultra- fine particles having particle size in nanometer (10^{-9} m) range, at least <100 nm. When the grain size of the material reduces to nano scale, the relative volume of the atoms in the grain boundary enhances and the ordered arrangement conditions of original atoms or molecules will be destroyed leading to alteration of many properties such as structural, micro structural, chemical and mechanical [61-62]. A small amount of nano particle addition in refractories has a great influence on its properties. Nano particles can disperse even among the tiny spaces between coarse, medium and fine particles of refractory raw materials thereby filling of interior pores and gaps and improve the microstructure and reactivity [15]. Nano materials not only absorb and relieve the stress due to thermal expansion and shrinkage of refractory particles but also reduce the mal-distribution of thermal stress in the interior portion of refractories [15]. Incorporation of nano particles also increases the strength and corrosion resistance of refractory at high temperature due to its high surface to volume ratio [15].

Addition of small amounts (~ 2 wt %) of nano –zirconia (ZrO_2) in dolomite refractories resulted in the improvement of densification, thermal shock resistance, slaking resistance and slag corrosion resistance [63]. Presence of nano iron oxide in $\text{MgO-Cr}_2\text{O}_3$ refractories facilitated the formation of magnesio ferrite spinel at lower temperatures which dramatically improves the properties of the bricks [64]. Addition of 0.4% nano Fe_2O_3 in silica refractories has improved the properties [65].

2.5 Role of nano carbon in low carbon MgO-C refractory:

Carbon containing refractories is widely used in various vessels of hot metal and molten steel because of their high durability owing to the high thermal conductivity and non-wettability of carbon. The nano carbon particles and resin binder disperse among the spaces between the coarse, medium and fine particles of the refractory raw materials. Additives as well as other miscellaneous materials consequently play a role by filling up the interior pores and gaps between the various particles. As a result, nano carbons not only absorb and relieve the stress due to thermal expansion and shrinkage of refractories particles but also reduce the mal-distribution of thermal stress in the inner portion of refractories. The refractories with an addition of only 1.5% nano carbon particles showed thermal spalling resistance equivalent to that of existing refractories containing 18% graphite [15]. The effect of addition of fine carbon particles such as nano carbon black to the matrix as a means to improve the spalling resistance is investigated. The modulus of elasticity showed a decrease with an increase in the fine carbon content and the amount of creep deformation found to decrease with an increase in fine carbon content. The measurement of change under load showed that the texture of MgO-C bricks changed less as the fine carbon content increased. This indicated that fine carbon addition would be effective in improving the spalling resistance of low carbon MgO-C brick, because it would suppress the sintering of MgO [66-68]. With the increase of nanometer carbon black added, the data of MOR and CCS of MgO-C specimens raised gradually. When the amount of carbon black reached up to 15 mass%, the values of MOR, HMOR and CCS of specimens increased up to 40%, 39% and 45% respectively compared with the samples without the addition of nanometer carbon black [69-71].

2.6 Objectives of the present studies:

The main objective of the present work:

The BOF is the overwhelmingly popular process selection for oxygen steelmaking and MgO-C refractories are widely used as working lining for BOF vessel. Combination of graphite with MgO increases resistance to thermal shock, controls thermal expansion, improves corrosion resistance, and decreases wettability with corrosive liquid phases. On the other hand, due to the increased demand for high quality steel such as API steel or ultra- low carbon steel, the carbon content in the MgO-C bricks have greater importance. The problems with conventional MgO-C brick are carbon pick up by steel and increase in heat loss, which has resulted in demand for low carbon MgO-C bricks. Reducing in the carbon content, however, may decrease the thermal spalling resistance, which is contributed to carbon's high thermal conductivity and low thermal expansion. The thermal spalling resistance of the said brick can be improved either by adjusting the particle size distribution or by additives. In this study we investigate the role of Nano Carbon for the development of low carbon MgO-C brick with better properties. For this study in this work amount of Nano-C was varied from 0.3 % to 1.5 % along with pitch and liquid resin as other source of Carbon. The results of the samples prepared were compared with the conventionally prepared MgO-C (10%) bricks. Finally the suitable anti-oxidant and the amount of anti-oxidants were fixed by a no. of experiments.

Chapter: 3
EXPERIMENTAL WORK

3.1 Raw materials:

Commercially available high quality with low impurity fused magnesia (FM), natural flakes graphite, aluminium metal powder (- 150 μm), boron carbide powder and nano carbon black were used to maintain the granulometry of the mixture. Liquid resin and pitch powder were taken as additives of base raw materials for fabrication of low carbon graded MgO-C brick.

In this present work, high purity magnesia, FM 97 was taken as the raw material for fused magnesia, considering the selection criteria like purity, CaO/SiO₂ ratio, low Fe₂O₃ content and large crystals in the range of 500-1500 μm [43, 45]. High purity graphite, 94 FC, was selected as a raw material for carbon and resol resin (novalac type) was used as binder. The physic-chemical properties of magnesia, flake graphite ,liquid resin and pitch powder and nano carbon black are are given in tables below.

Table.3.1: Chemical composition in percentage of fused magnesia:

Chemical composition						
Raw materials -----	MgO	Al ₂ O ₃	SiO ₂	CaO	Fe ₂ O ₃	Na ₂ O
Fused magnesia	97.35	0.07	0.40	1.40	0.50	0.50

Table:3.2 : Physical and chemical analysis of flake graphite

Raw materials	carbon (%)	volatile matter (%)	Ash (%)	Surface area(m ² g ⁻¹)
Flake graphite	94.1	0.80	5.08	6.37

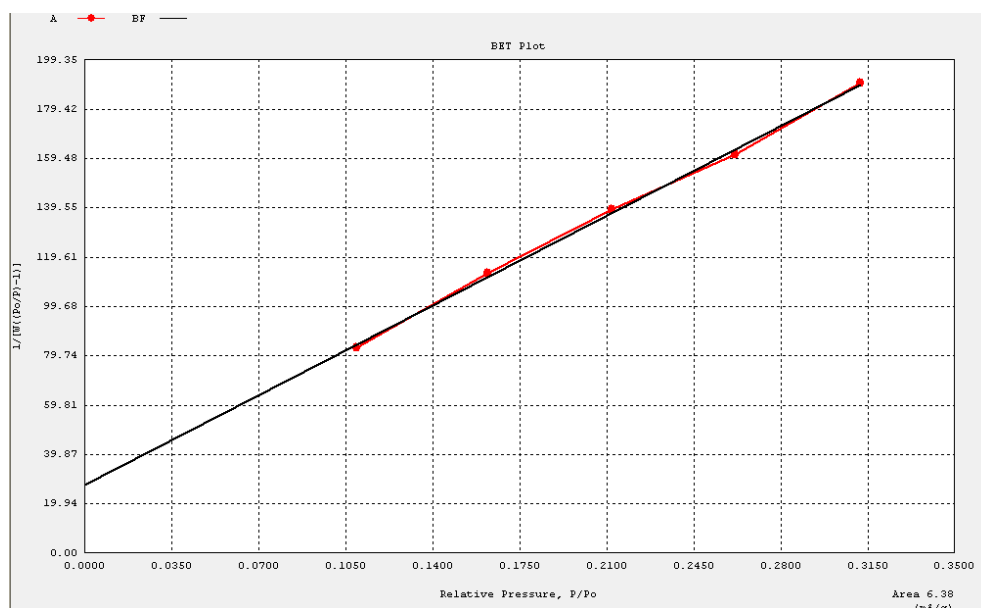


Fig.3.1 :BET surface area graph of graphite.

Table.3.3: Physical and chemical analysis of Pitch powder

Raw materials	Carbon (%)	Volatile material (%)	Ash (%)	Softening pt ($^{\circ}\text{C}$)
Pitch powder	52	47	1.4	135

Table.3.4: Physical and chemical analysis of liquid resin

Property	Liquid Resin
Viscosity (CPS) at 25 $^{\circ}\text{C}$	8500-9000
Specific gravity at 25 $^{\circ}\text{C}$	1.23
Non- volatile matter (%)	80.10
FixedCarbon (%)	47.85
Moisture (%)	~ 4.0

Table.3.5: Physical and chemical analysis of nano carbon black

Raw materials	carbon (%)	volatile matter (%)	Ash (%)	Surface area(m ² g ⁻¹)
Nano carbon black	98.09	1.52	0.39	116.5

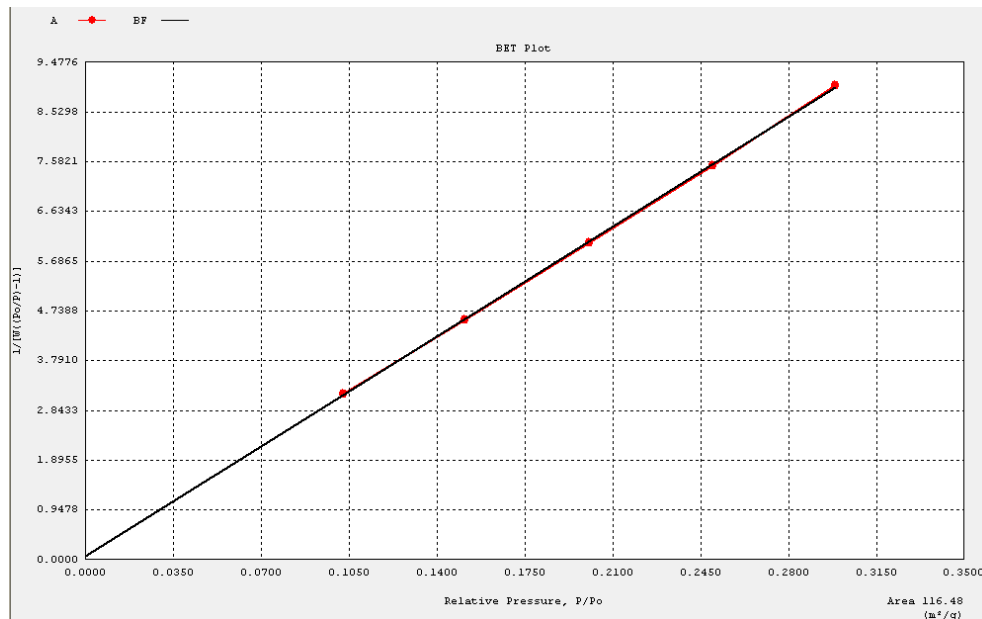


Fig.3.2: BET surface area of nano carbon black

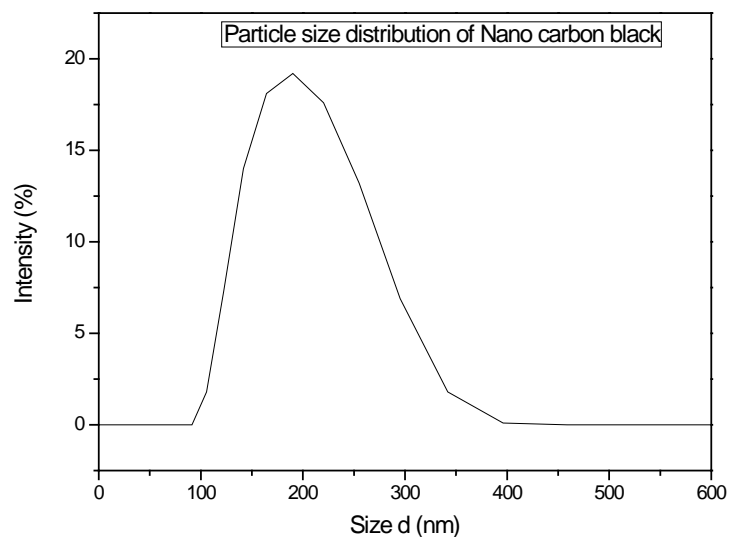


Fig3.3: Particle size distribution of nano carbon black.

Aluminium powder:

% Aluminium=98

Particle size: 100% passing through 150 BSS, 50-70% passing through 300 mesh BSS

Boron carbide:

% B₄C=95%, total Boron=77wt%, Total carbon=21wt %, (Fe₂O₃, B₂O₃)traces

Particle size:-100BS=100% min, -200BS =95wt% min, 300BS=75% min.

3.2 Determination of granulometry:

Different size raw materials are taken for manufacturing of any refractory brick to obtain a higher packing density. If only coarser particles are used minimum shrinkage value will occur but porosity will remain as inter-granular voids between the coarser particles. Hence for better filling the pores between different coarser refractory grains, the fine particles are also essential. Again higher amount of fine particles than required results in decrease in density and increase of coarse particles results in segregation. So to achieve better property of the bricks, the particle size distribution is very much essential. Granulometric study is required for better particle packaging that will give better green density. This study can be done on two basic aspects of particles packing; one is the measurement of the density as loose condition, termed as loose filled density and the secondly as tapped density. The following flow-sheet provides the method of measuring these densities.

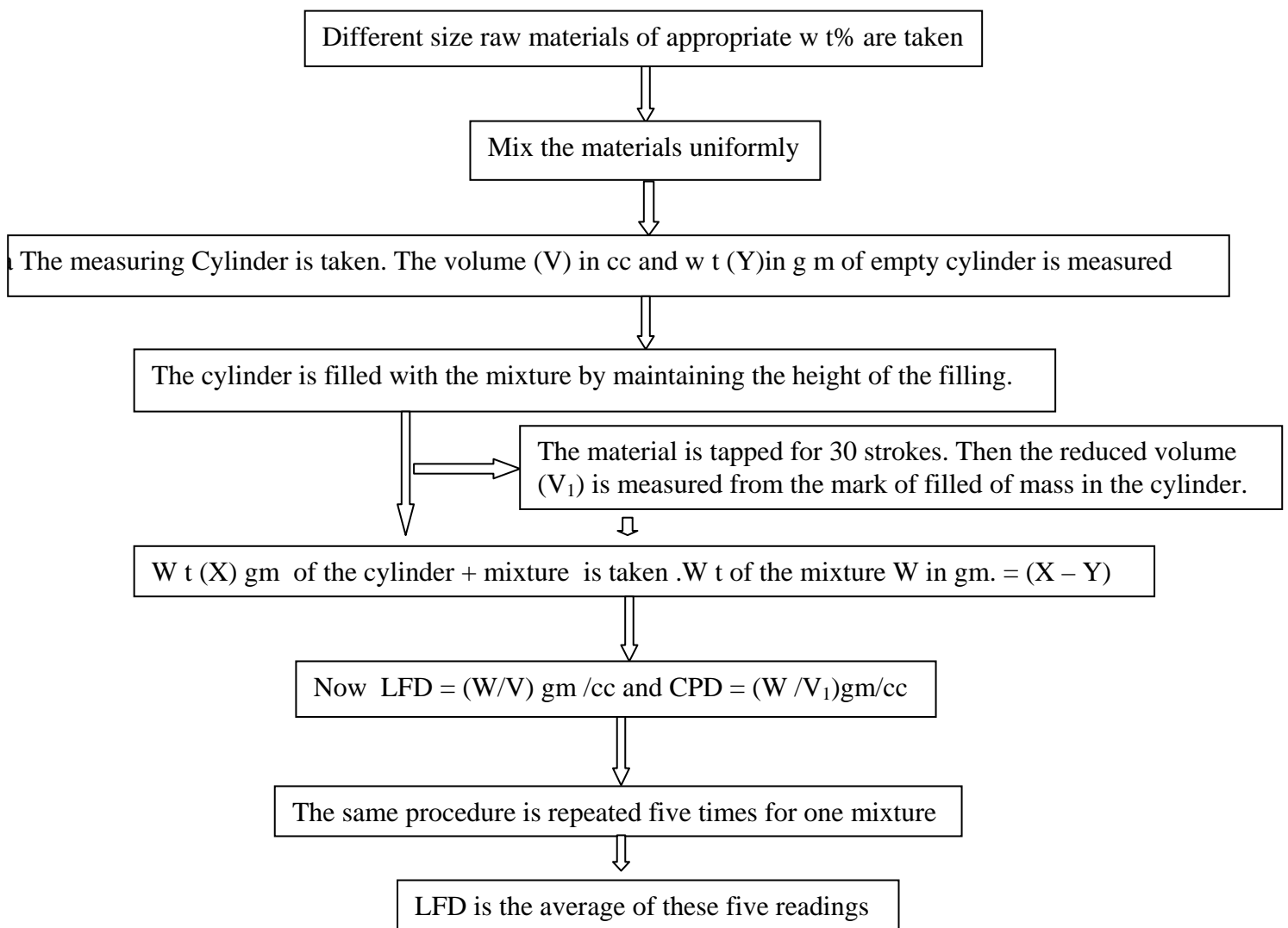


Fig.3.4: Flow chart of determination of granulometry.

Next the green density has been done by varying the pressing pressure on the granulometric composition that has resulted in the highest tapped density. The trial green density batch was prepared as per the process of mixing, ageing and pressing method (described in detail later) and was pressed at different specific pressures. The optimum pressure was determined by measuring the green density of the pressed samples. Specific pressure that gives the highest green density was selected as the optimum one and was used for all the different compositions studied in this work.

3.3 Fabrication of low carbon MgO-C brick:

Batch preparation:

Different compositions of MgO-C bricks have been fabricated first by varying nano carbon content starting from 0 to 1.5 with a fixed graphite content of 3% and then for a particular nano carbon content the graphite content was varied starting from 1 to 9 %.And finally some study has been done on the effect of antioxidant contents. All the variations done in the study are compared with the conventionally used MgO-C brick composition prepared under similar conditions. All the different batch compositions of MgO-C brick done in the present study are given in the following tables.

Table3.6: Batch composition of MgO-C varying nano carbon for a particular percentage of graphite.

Raw materials	T-1	T-2	T-3	T-4	T-5	T-6	T-C
MgO	96	96	96	96	96	96	89
Graphite	3	3	3	3	3	3	10
Nano carbon	0	0.3	0.6	0.9	1.2	1.5	0
Resin	2.75	2.75	2.75	2.75	2.75	2.75	2.75
Pitch	1	1	1	1	1	1	1
Al metal powder	0.5	0.5	0.5	0.5	0.5	0.5	0.5
B ₄ C	0.5	0.5	0.5	0.5	0.5	0.5	0.5

Table3.7: Batch composition of MgO-C varying graphite content for a particular percentage of nano carbon.

Raw materials	T-7	T-8	T-9	T-10	T-11	T-C
MgO	98	96	94	92	90	89
Graphite	1	3	5	7	9	10
Nano carbon	0.9	0.9	0.9	0.9	0.9	0
Resin	2.75	2.75	2.75	2.75	2.75	2.75
Pitch	1	1	1	1	1	1
Al metal powder	0.5	0.5	0.5	0.5	0.5	0.5
B ₄ C	0.5	0.5	0.5	0.5	0.5	0.5

Table.3.8: Batch composition of MgO-C varying anti -oxidant content for 0.9wt% of nano carbon and 5wt% of graphite.

Raw materials	T-12	T-13	T-14	T-15	T-C
MgO	94	94	94	94	89
Graphite	5	5	5	5	10
Nano carbon	0.9	0.9	0.9	0.9	0
Resin	2.75	2.75	2.75	2.75	2.75
Pitch	1	1	1	1	1
Al metal powder	0	0.5	0.75	1	0.5
B ₄ C	0	0.5	0.25	0	0.5

Table.3.9: Batch composition of MgO-C varying anti -oxidant content for 0.9wt% of nano carbon and 3wt% of graphite

Raw materials	T-16	T-17	T-18	T-19	T-C
MgO	96	96	96	96	94
Graphite	3	3	3	3	5
Nano carbon	0.9	0.9	0.9	0.9	0.9
Resin	2.75	2.75	2.75	2.75	2.75
Pitch	1	1	1	1	1
Al metal powder	0.0	0.50	0.80	0.75	0.5
B ₄ C	0.0	0.50	0.20	0.25	0.5

Mixing:

The purpose of mixing the raw materials is to make a refractory batch and transform all the solid components and the liquid additions into a macro homogeneous mixture that can be subsequently molded or shaped by one of the numerous fabrication methods employed by modern refractory manufacturers. All the raw materials were thoroughly mixed using pan mixer at room temperature for nearly 45 minutes. Table shows the mixing sequence of various raw materials.

Table.3.10: Mixing sequence of MgO-C bricks

Steps	Mixing sequence	Mixing time (Min)
1	(Coarse + Medium) MgO+ Graphite+ Aluminium metal powder +Hard pitch powder + Nano carbon black	4
2	Addition of liquid resin	8
3	Addition of fines MgO powder	28

Aging:

After mixing, the mixture is allowed to stay for 2 hour for aging. This helps for polymerization of carbon to take place by carbon- carbon interlocking mechanism.

Pressing:

The mixed materials after aging were compacted to give a desired shape by pressing. The Bricks dimension were 220 mm×110 mm×75 mm. The aged mixtures were pressed uniaxially by hydraulic press in a steel mould. After calculating the volume of the mould the appropriate amount of mixture was taken maintaining a green density obtained in the trial batch. The steel mould was cleaned using cotton and brush after each pressing. To avoid stickiness between the mixture and mould kerosene was used as a lubricating agent. The mixture was added slowly into the mould with bottom punch. To achieve better filled density and uniform leveling the mixture was tapped slowly into the mould. Then the top punch was applied slowly. First the pressing was done uniaxially with a low pressure of 0.5 ton / cm². It was allowed to hold for 60 seconds and then the pressure was decreased slowly to remove the entrapped air inside the mixture. This process is called Dearing and is done to avoid the lamination in the brick. Finally the mixtures were pressed with a specific pressure of 2 ton/cm² using hydraulic press (SACMI, Italy) with 12 strokes. For the pressed samples lamination was checked critically.

Tempering:.

Tempering is the heat treatment process of the refractories at low temperature to remove volatiles from the organic green binders and to impart enough green strength. By this process the chemical bond is developed in the refractory body. Phenolic resin converts to brittle solid mass called resist during curing process (above 200° C.) and then with increasing the temperature it converts to carbonaceous phase (residual carbon) which is responsible for the final carbon binding and strength development in such structures. However certain drawbacks of residual carbon of phenolic resin cause limiting applications of phenolic resin as binding agent. The pressed samples were tempered at 200 °C for 12 hour in a tempering kiln.

Coking:

The samples were cut in different sizes for different testing purposes from the cured brick and were dried at 100 °C after wet cutting. Coking was carried out at 1000 °C for 4 h under reducing atmosphere (carbon bed).

The physical & mechanical properties of the different compositions after tempering and after coking were characterized using different instrumental techniques.

3.4 General characterization:

3.4.1 Surface area:

Surface area was determined using Brunauer-Emmett-Teller (BET) method by using a surface area analyzer (Quantachrome, USA). The measured surface area was converted to equivalent particle size according to the equation:

$$\text{Size}_{\text{from BET}} = (6000/\text{density} \times \text{surface area}).$$

3.4.2 Particle size distribution:

The particle size analysis is very important for the work using nano-carbon. In order to find out the particles size distribution, the nano carbon and graphite was dispersed in water by ultrasonic processor [Oscar Ultrasonic] for 10 minutes. Then experiment was carried out in computer controlled particle size analyzer MALVERN MASTER SIZER (UK). The dispersant used in this case was sodium hexa meta phosphate. The particle diameters vs. cumulative volume % graphs for different raw materials were drawn by the software.

3.4.3 Apparent porosity (AP) and Bulk density (BD) :

AP is defined as ratio of the total volume of the closed pores to its bulk volume and expressed as a percentage of the bulk volume. Closed porosity are the pores that are not penetrated by the immersion liquid, whereas open porosity are the those pores which are penetrated by the immersion liquid. AP was measured as per the standard of IS: 1528, Part-8(1974) both for tampered and coke samples. The Archimedeian evacuation method generally measures both bulk density and apparent porosity.

The test specimen of 65 mm × 65mm × 40 mm is taken and dried at 100 °C after wet cutting. After taking the dry weight (W_1) it is placed in empty vacuum desiccators and subjected to vacuum of less than 25 mm of mercury column for 30 minutes. Then the water is allowed to enter and vacuum is maintained for 20 minutes. This process is planned to fill up all voids present in the specimen with water. The suspended weight (W_2) and soaked weight (W_3) are taken.

$$\text{A.P} = (W_3 - W_1 / W_3 - W_2) \times 100$$

BD is the ratio of the mass of the dry material of a porous body to its bulk volume expressed in g/cm^3 or kg/m^3 , where bulk volume is the sum of the volumes of the solid material, the open pores and the closed pores in a porous body. BD was measured as per the standard of IS: 1528, Part -12 (1974) both for tampered and coke samples.

Whereas true density is the ratio of mass of the material of a porous body to its true volume and true volume is the volume of solid material in a porous body.

$$\text{B.D} = (W_1/W_3 - W_2) \times \text{density of liquid at temperature of test}$$

(e.g. density of water at 25°C : 0.997044, at 30°C : 0.995646 g/cc)

Each value of AP and BD represented here was of the average of five parallel samples.

3.4.4 Cold Crushing Strength:

Cold crushing strength of refractory bricks and shapes is the gross compressive stress required to cause fracture. It was measured as per ASTM C-133 for both tempered and coke samples. The test specimen of $65 \text{ mm} \times 65 \text{ mm} \times 40 \text{ mm}$ is taken and dried at 100°C after wet cutting. Cold crushing strength of the refractories are measured by placing a suitable refractory specimen on flat surface followed by application of uniform load to it through a bearing block in a standard mechanical or hydraulic compression testing machine. The load at which crack appears in the refractory specimen represents the cold crushing strength of the specimen. The load is applied uniformly on the sample in the flat position. It is expressed as (Kg/cm^2) .

The working formula for calculating CCS is given by

$$\text{CCS} = \text{Load} / \text{Area}$$

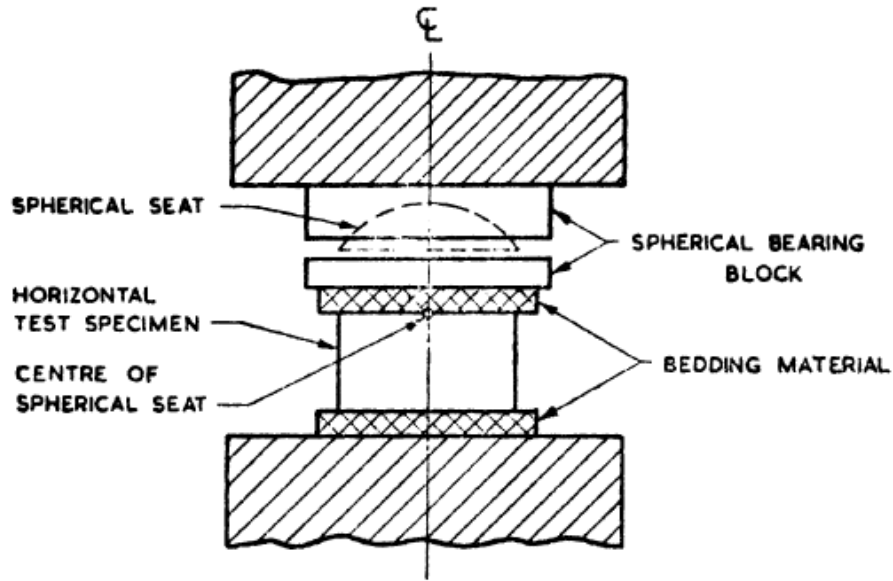


Fig3.5: - Schematic diagram for CCS

3.4.5 Hot modulus of rupture (HMOR):

The modulus of rupture of refractory specimen is determined as the amount of force applied to a rectangular test piece of specific dimensions until failure occurs. This test method covers the determination of the modulus of rupture of carbon-containing refractories at elevated temperatures in air. It was determined as per ASTM C133-7. Each value of HMOR was the average of five parallel specimens. It was done by three-point bending test using HMOR testing apparatus (Netzsch 422, Germany). All the specimens for HMOR were taken as 150 mm × 25 mm × 25 mm and dried at 100 °C after wet cutting, without pre-firing at air atmosphere. The final temperature of HMOR was 1400 °C with a heating rate of 5 °C/min. It was done in air atmosphere with a soaking time of 30 min. Finally, the loading rate of HMOR was 0.15 MPa/s. It is done in the machine NETZSCH.

The HMOR value was calculated by the following formula:

$$\text{HMOR} = (3 W \times L) / (2 b \times d^2)$$

Where “W” (kg) is the maximum load when the specimen is broken;

“L” is the span length between the lower supporting points. (120 mm for all the tests in the work)

“b” is the breadth (cm), “d” is the height of the specimen (cm).

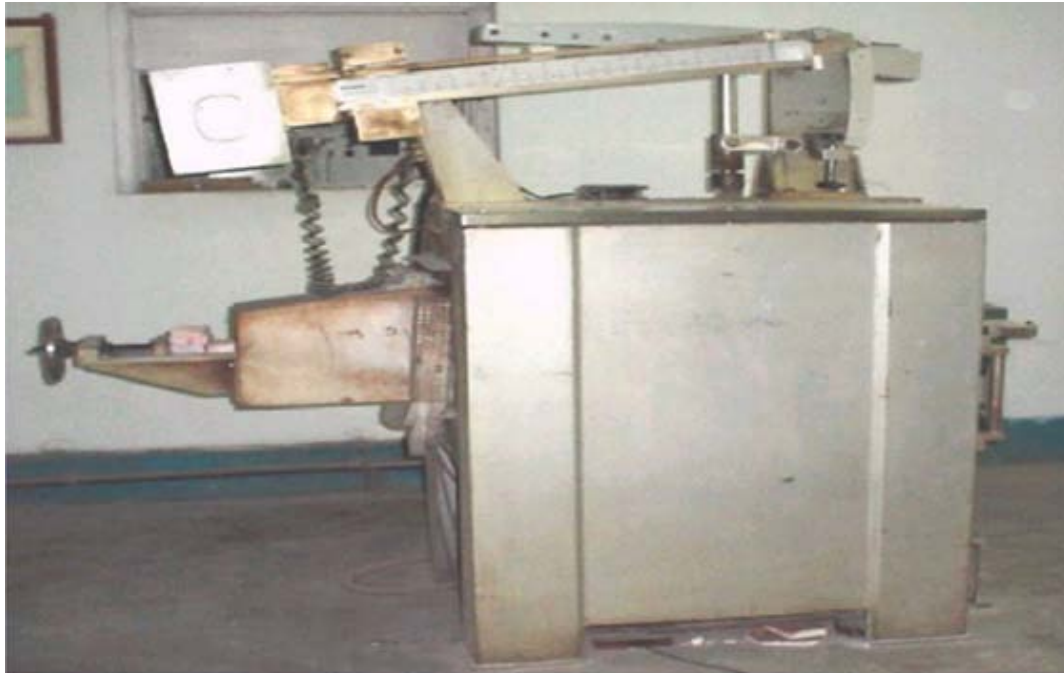


Fig.3.6: HMOR machine

3.4.5 Modulus of elasticity (MOE):

MOE was measured by the ultrasonic method in which the propagation speed of ultrasonic waves was measured along the length of tempered samples of 150×25×25 mm.

Ultrasonic pulse velocity testing (UPVT) was first reported being used on refractory materials in the late 1950's. Briefly, pulses of longitudinal elastic stress waves are generated by an electro-acoustical transducer that is held in direct contact with the surface of the refractory under test. After travelling through the material, the pulses are received and converted into electrical energy by a second transducer.

Most standards describe three possible arrangements for the transducers:

- (1) The transducers are located directly opposite each other (direct transmission).
- (2) The transducers are located diagonally to each other; that is, the transducers are across corners (diagonal transmission).
- (3) The transducers are attached to the same surface and separated by a known distance (indirect transmission).

The velocity, V , is calculated from the distance between the two transducers and the electronically measured transit time of the pulse as

$$V \text{ (m/s)} = L / T$$

Where L is path length (m) and T is transit time (s).

By determining the bulk density, the Poisson's ratio and ultrasonic velocity of a refractory material, it is possible to calculate the dynamic modulus of elasticity using the equation below:

$$MOE = V^2 \rho \left(\frac{(1 + \nu)(1 - 2\nu)}{(1 - \nu)} \right)$$

Where

V is the pulse velocity (m/s),

ρ is the bulk density (kg/m³) and

ν is the Poisson ratio.

The transducers were rigidly placed on two parallel faces of the rectangular sample of 150×25×25 mm. Vaseline grease is used as the coupling medium. The ultrasonic velocity was then calculated from the spacing of the transducers and wave form time delay on the oscilloscope.

3.4.6 Oxidation resistance:

For oxidation resistance test, cylindrical samples (height =50 mm, diameter =50mm) were prepared by wet cutting from the tempered bricks and then dried at 100 °C. These cylinders were placed in an electrically heated furnace (heating rate of 5 °C /min) under ambient condition at 1400 °C for 5 h. The furnace is then cooled down at the same rate of 5 °C /min. Fired samples were horizontally cut into two pieces. Then the black surface remaining was measured at eight different locations. The total diameter of the samples also noted. The average value was taken.

$$\text{Oxidation index} = (\text{Oxidized diameter} / \text{Total diameter}) \times 100$$

3.4.7 Static slag corrosion test:

Slag corrosion test by static crucible method was done for all the different compositions at 1650 °C for 4 h with steel making ladle slag. Chemical composition (%) and basicity of the steel making ladle slag are given in table. The sections after slag attack are visually compared and corrode dimensions were taken.

Table.3.11: Chemical composition (wt %) and basicity of the steel making ladle slag.

CaO (wt%)	SiO ₂ (wt%)	Al ₂ O ₃ (wt%)	MgO(wt%)	Fe ₂ O ₃ (wt%)	MnO(wt%)	CaO/SiO ₂
37.5	12.48	12.08	6.95	30.00	0.99	3.00

3.4.8 Thermal shock resistance:

Thermal shock /thermal spalling is the direct result of exposing the refractory installations to rapid heating and cooling conditions which cause temperature gradients within the refractory. Such gradients cause an uneven thermal strain distribution through the sample, may cause failure of the material [72-73]. The standard method of finding out spalling resistance is heating the material at an elevated temperature followed by sudden cooling in air at ambient temperature. The thermal shock resistance of refractory materials is determined using standard quench tests [74-75] in which the material is heated and cooled subsequently and the number of heating & cooling cycles that a material can withstand prior to failure is taken as its thermal shock resistance. The quantification was done by the number of cycles to withstand such temperature fluctuations. The sample specimen of 30mm×40mm×40mm were taken and dried at 100 °C after wet cutting. These samples are heated at 1400°C for 10 minutes and then suddenly brought down to ambient condition by cooling it in air for 10 minutes. The number of cycles before any crack in the specimen was noted down as the spalling resistance. The testing was correlated to ASTM C-1171.

3.4.9 Pore size distribution:

The test samples (cube shape of 10 x 10 x 10 mm³) were cut from the tempered bricks, dried at 110 °C for 3 h and cooled in desiccators. The test samples were then placed in pycnometer which was inserted in the part of the mercury porosimeter sample holder with a vacuum level of 50µm Hg. Mercury porosimeter has been used to test the samples with a maximum pressure of 33000 psi. Surface tension and contact angle of mercury was 485 dynes/ cm² and 130 ° respectively. Pore size distribution pattern i.e. open pore volume available for 'Hg' intrusion under pressure with respect to the pore diameter has been characterized.

3.4.10 Microstructure:

Thin slices of samples were polished by various grades of abrasive papers and diamond paste. The microstructures of these samples were done using scanning electron microscopy (SEM, model JSM 6480 LV JEOL, Japan).

Chapter 4:
RESULTS AND DISCUSSION

4.1 Determination of particle size distribution by loose field density and closed packed density:

The measurements of loose field density and close pack density procedure are described in chapter 3. The table below shows the different values of L.F.D and C.P.D depending upon the different MgO percentage.

Table.4.1: Determination of granulometry:

Serial no:	Fused MgO (wt %)	L.F.D	C.P.D
1	(4-6) mm 11 wt% (1-4)mm 43 wt% (0-1)mm 31 wt% Fine 11wt%	0.246	0.261
2	(4-6) mm 10 wt% (1-4)mm 40 wt% (0-1)mm 25 wt% Fine 21wt%	0.240	0.270
3	(4-6) mm 10 wt% (1-4)mm 40wt% (0-1)mm 29 wt% Fine 17wt%	0.237	0.269
4	(4-6) mm 10 wt% (1-4)mm 40wt% (0-1)mm 30 wt% Fine 16wt%	0.243	0.274

So it is observed that serial no: 4 gives the maximum L.F.D and C.P.D. So for the entire work for all batches, the granulometry of serial no: 4 was followed.. It is due to the better filling of pores between different MgO aggregate.

4.2 Physical and chemical properties of nano carbon added low carbon MgO-C bricks by varying the nano carbon percentage and compared with 10% graphite containing MgO-C brick:

4.2.1 Apparent porosity, Bulk density and Cold crushing strength (Before and after coking):

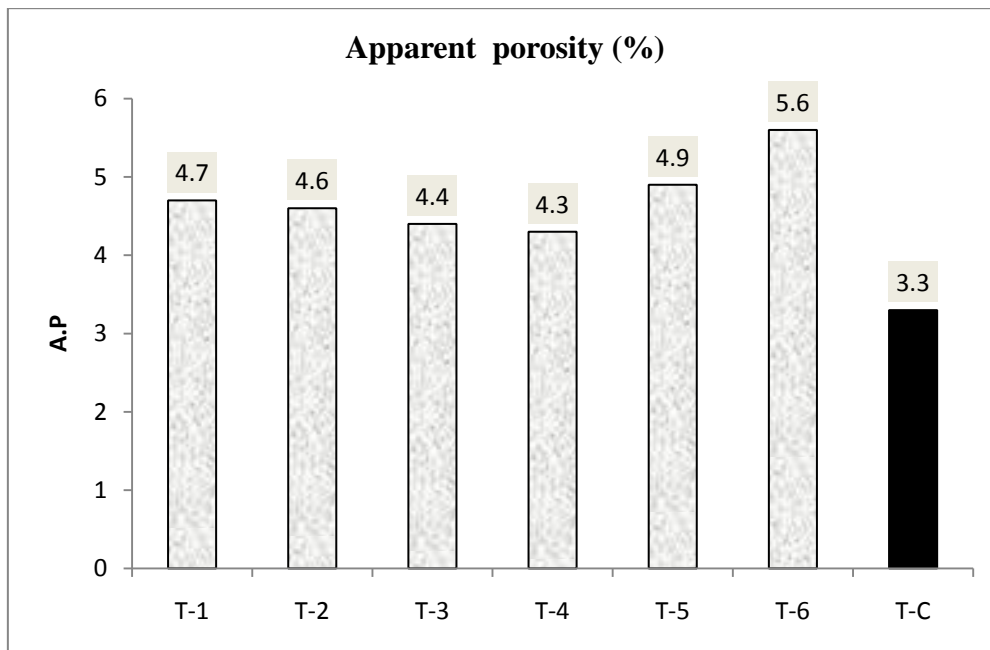


Fig.4.1: variation of apparent porosity with the variation of nano carbon content.

The change in AP with the increase of nano carbon is shown in fig.4.1. With the addition of nano carbon the percentage of AP is reducing linearly upto 0.9wt% nano carbon. The AP varies in the range of 4.7 to 5.6 wt % .AP has the value of 4.7 wt% without any nano carbon and has the value 4.3 for o.9 wt% nano carbon. This is because of addition of nano carbon increases the filling of spaces between many refractory particles .Thus overall reducing the porosity. But after 0.9 wt% with the increase of nano carbon percentage increases the AP. The value of AP is even greater for without nano carbon. This is because upto 0.9 wt% nano carbon the pores are almost filled up by the nano carbon. So over 0.9 wt% nano carbon, further filling is not possible .So further increase of nano carbon in the matrix increases the porosity of the brick. Whereas the AP value for conventional brick is much lower and have a value 3.3%.This is because the conventional brick contains 10 wt% graphite. The graphite being a filling material it decreases the porosity.

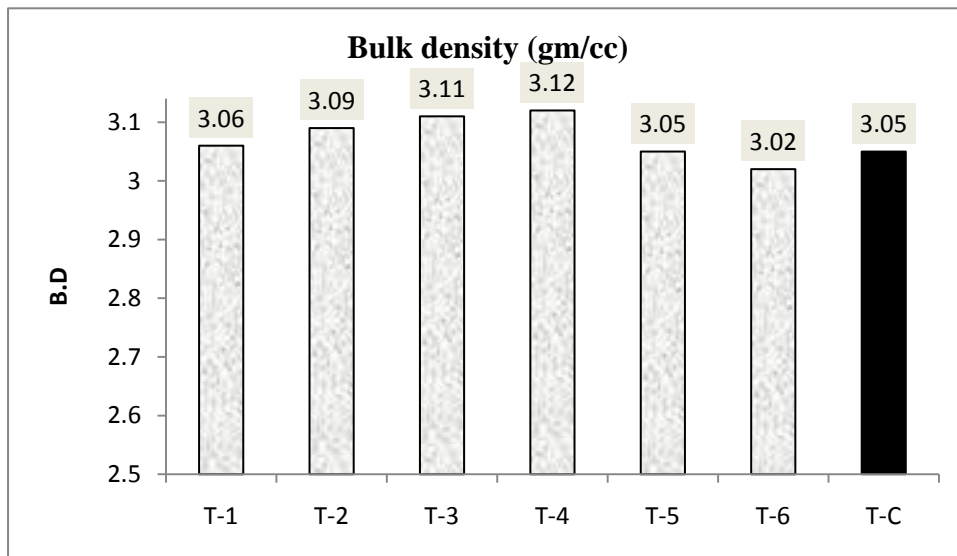


Fig.4.2:variation of bulk density with the variation of nano carbon content.

The variation of bulk density is shown in fig:4.2. The variation of bulk density with the nano carbon is very less, it ranges from 3.06 to 3.12. The BD without the nano carbon was 3.06. Then with the increase of nano carbon content better pore filling is done, results in a higher B.D. It has the value of 3.12 gm/cc for 0.9 wt% nano carbon. But further increase of nano carbon no further filling is occurred. It only increases the overall sample volume and results in a decrease in BD.

The BD for conventional brick is 3.05 gm/cc whereas for 0.9 wt% nano carbon containing bricks have the value of 3.12 gm/cc. So nano carbon containing brick had better BD than the conventional brick.

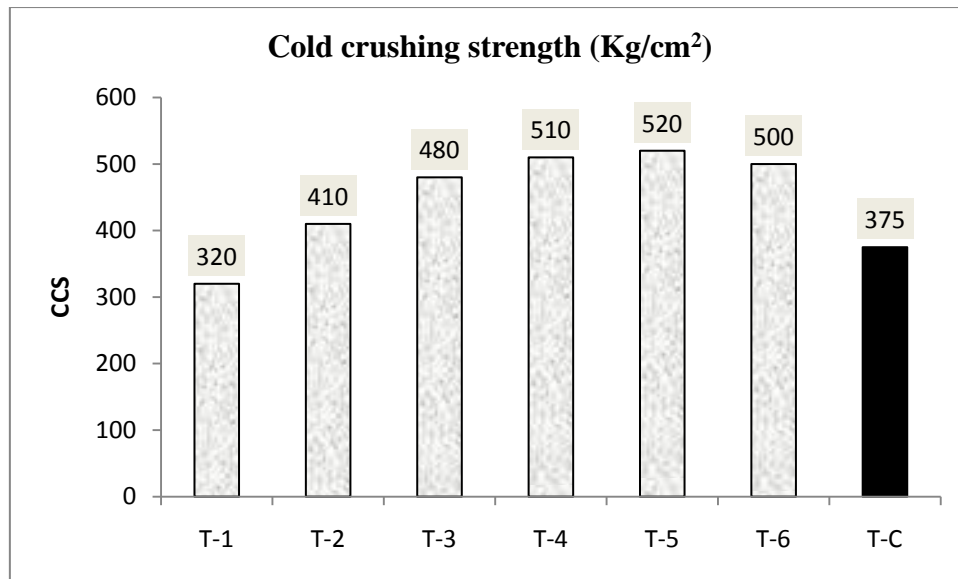


Fig.4.3: Variation of cold crushing strength with the variation of nano carbon content.

The variation of cold crushing strength with the nano carbon % is shown in fig:4.3 . It is clearly shown in figure that the CCS values increases linearly with the nano carbon percentage. Without nano carbon the CCS value is 320 kg/cm² but for 0.9 wt % nano carbon added brick the value is 510 kg/cm² .It is almost 1.5 times greater than that of without nano carbon. This is because of the increase of nano carbon causes better filling of pores, results in an increase in BD. Thus CCS also increases. But CCS remain almost same after 0.9 wt% nano carbon added brick. This is because that the pore filling is achieved nearly the optimum value for 0.9 wt% nano carbon. So CCS remains nearly unchanged after 0.9% nano carbon. The CCS value of conventional brick is much lower than the 0.9 wt% nano carbon added low carbon containing MgO-C brick.

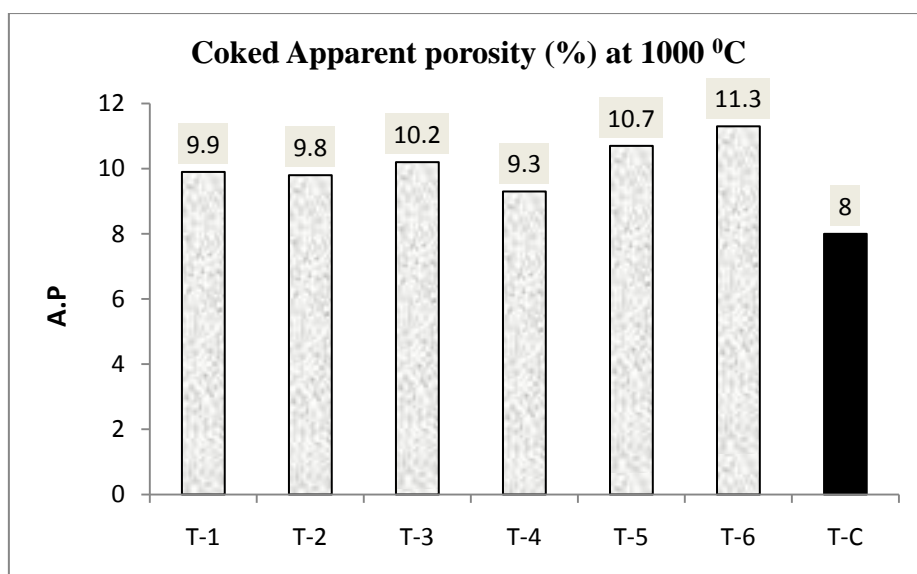


Fig.4.4: variation of coked apparent porosity with the variation of nano carbon content.

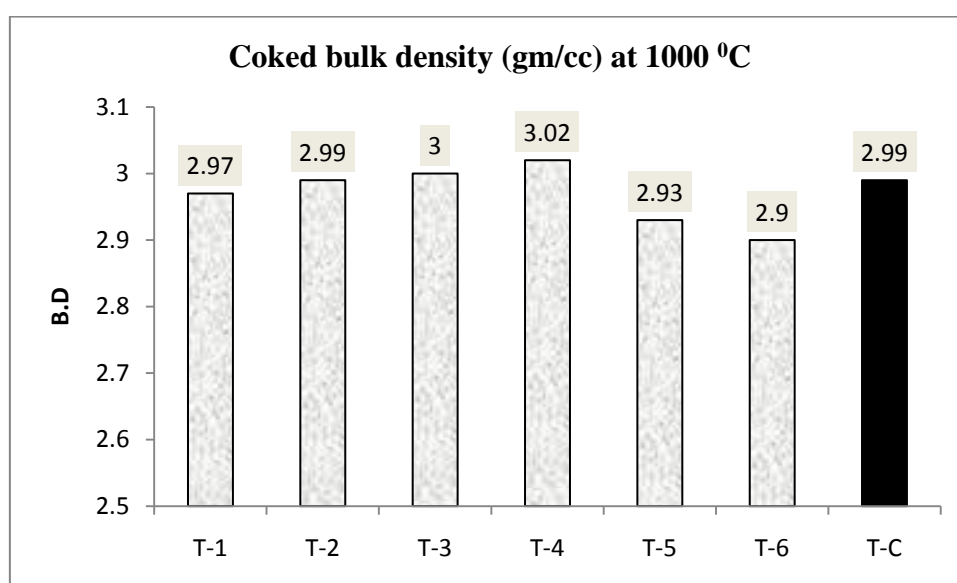


Fig.4.5: Variation of coked bulk density with the variation of nano carbon content.

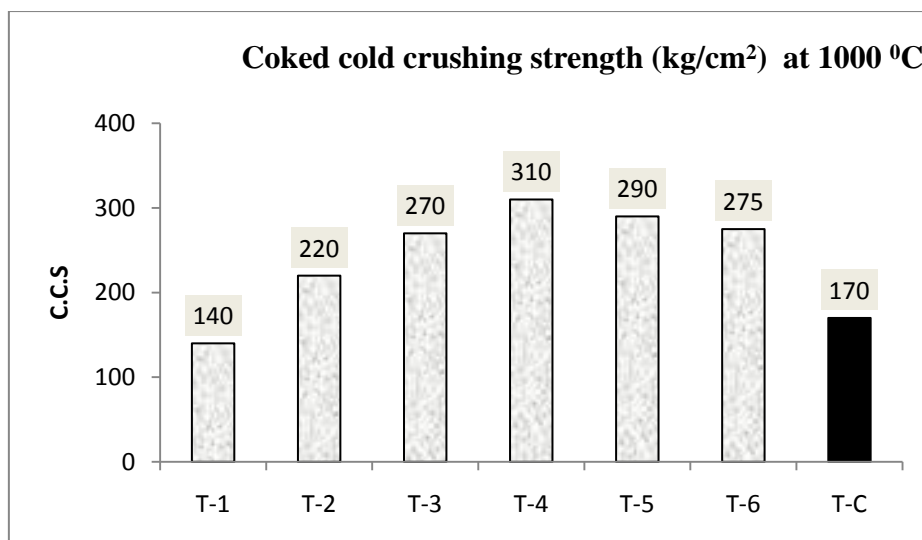


Fig.4.6: Variation of coked cold crushing strength with the variation of nano carbon content.

The coked AP, BD and CCS values are shown in fig:4. 4, fig:4.5 and fig:4.6 respectively. The coked AP,BD and CCS values changes in the same fashion as that of before coking. The coke AP, BD and CCS values are lowered because of the breaking of the interlocking texture that has been created after polymerization of phenolic resin. The breaking of the interlocking texture was due to the burning out of the total organic portion of resin and release of harmful decomposition gases such as benzene, toluene, phenols and xylene.

4.2.2 Hot modulus of rupture:

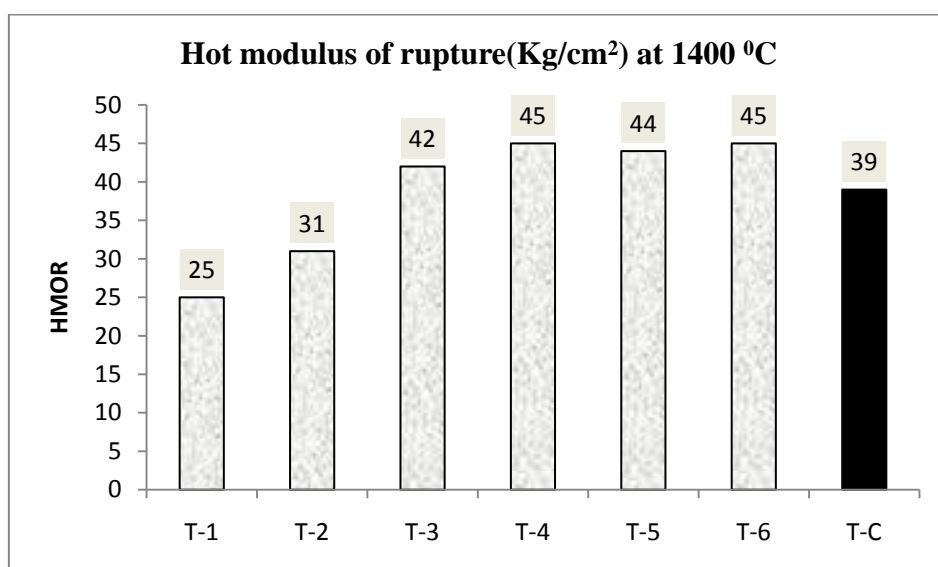


Fig.4.7: variation of hot modulus of rupture with the variation of nano carbon content.

Fig: 4.7 shows the variation of HMOR values with the increase of nano carbon. HMOR values also increases linearly with the nano carbon content and then remain almost constant after 0.9 wt% nano carbon containing brick. Without nano carbon HMOR has the value of 25 kg/cm² and 0.9 wt% nano carbon added brick has the maximum value of 45 kg/cm². With the increase of nano carbon better filling as well as better compaction is done. This results in a better strength. Nano carbon being very reactive it forms carbide at a higher rate. But at high temperature the increase of nano carbon content increases the carbide formation. Thus the HMOR values increases with the increase of carbide formation. But above 0.9% nano carbon no further betterment is achieved. It may be increase of formation of carbide and increase of oxidation of carbon resulting porous structure nullifying each other's effect. The HMOR value of conventional brick is 39kg/cm² which is lower than that of 0.9 wt% nano carbon added MgO-C brick. As the graphite content of conventional brick is much higher so the chances of oxidation of conventional brick are also higher. Oxidation results in a porous structure in the sample .Thus it reduces the HMOR values.

4.2.3 Oxidation resistance:

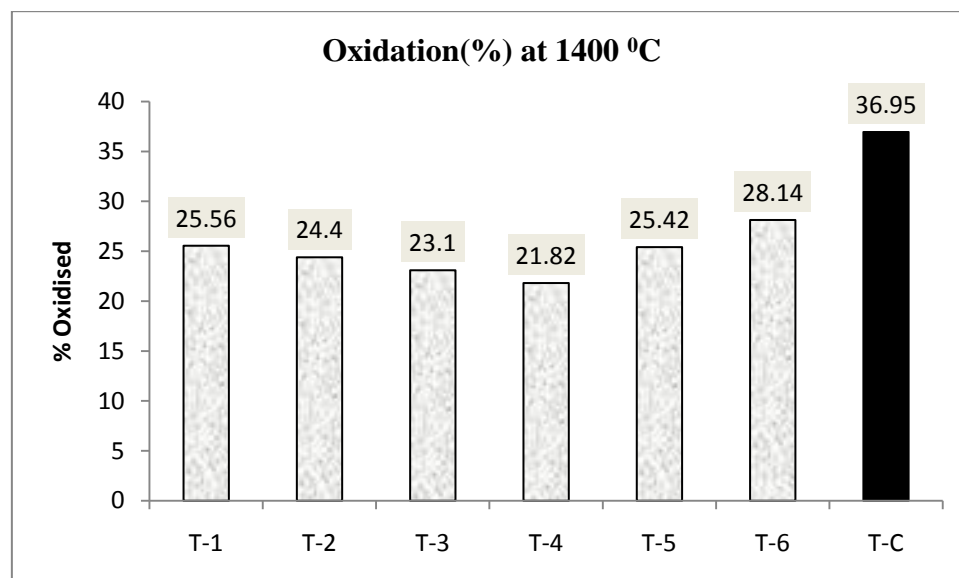


Fig.4.8: variation of oxidation resistance with the variation of nano carbon content.

The oxidation resistance values are shown in fig:4.8. With the increase of nano carbon the oxidation resistance increases. The oxidation resistance of without nano carbon has a value of 25.56%. The value decreases with the increase of nano carbon and has a value of 21.82 for 0.9 wt% nano carbon. Nano carbon being very reactive in nature, with the increase of nano carbon the percentage of carbide formation also increases. As carbides are having better oxidation resistance than free carbon or nano carbon, it increases the oxidation resistance. But above 0.9 wt% oxidation increases, it may be associated with no further carbide formation or higher oxidation for higher % of nano carbon as also for HMOR.

4.2.4 Modulus of elasticity:

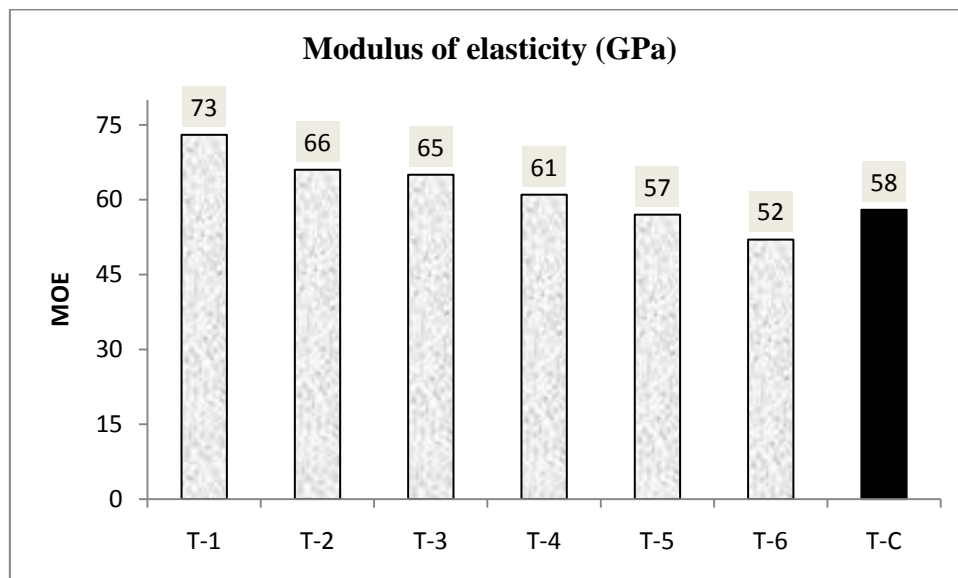


Fig.4.9: Variation of modulus of elasticity with the variation of nano carbon percentage.

Fig:4.9 describes the variation of MOE with the variation of nano carbon percentage. It is clearly shown that with the increase of nano carbon percentage MOE decreases almost linearly. In T-1 where there is no nano carbon and only 3 wt% graphite is there the MOE value is very high. But in the batch T-6 there is 3 wt% graphite and also 1.2 wt% nano carbon and shows a large decrease in MOE in compared with the T-1. 10 wt% graphite containing T-C shows also a lower value of MOE in compared with the 3 wt% graphite containing nano carbon added batches. As the graphite content increases so due to the compressibility of graphite, MOE value decreases.

4.2.5 Summary:

It is observed that from the batches of T-1 to T-6, the batch T-4 containing 0.9wt% nano carbon shows better result for most of the properties. So for next study of graphite content variation the nano carbon content was kept 0.9wt%.

4.3 Physical and chemical properties of nano carbon added low carbon MgO-C bricks by varying the graphite percentage for a fixed nano carbon and compared with 10% graphite containing MgO-C brick:

4.3.1 Apparent porosity, Bulk density and Cold crushing strength (Before and after coking):

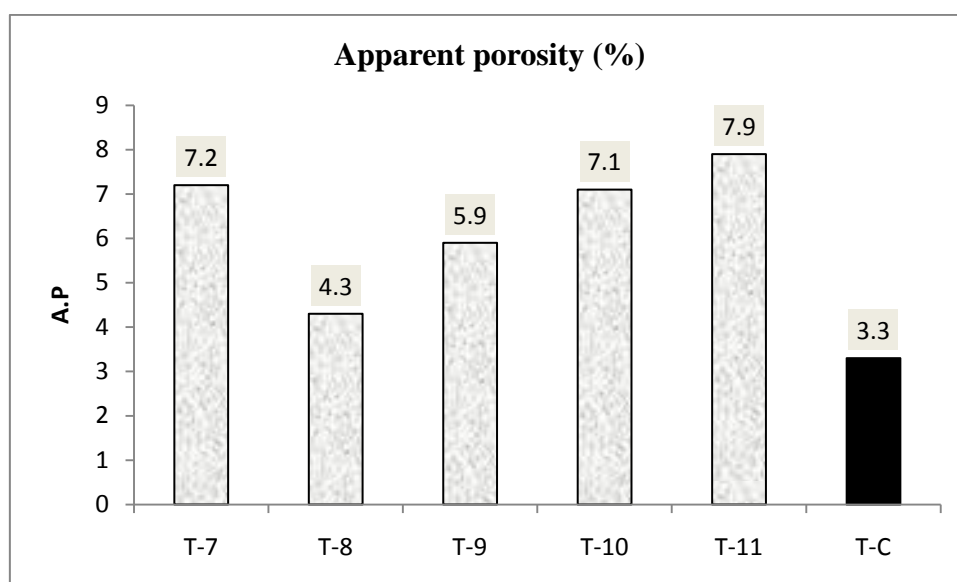


Fig.4.10: variation of apparent porosity with the increase of graphite content.

The variation of AP with the graphite content is shown in fig:4.10. From figure it is clear that with the increase of graphite content the AP decreases sharply. Sharp fall from 7.2 to 4.3 in AP is observed on increase of graphite content from 1 to 3 wt% due to the filling of pores of MgO aggregates by fine graphite powders. Further increase of graphite content increases the AP. This may be due to the lesser filling of voids at higher percentage of graphite, resulting in a relatively porous structure. The AP values are much higher than the conventional MgO-C sample. This is due to the higher volume of nano carbon percent.

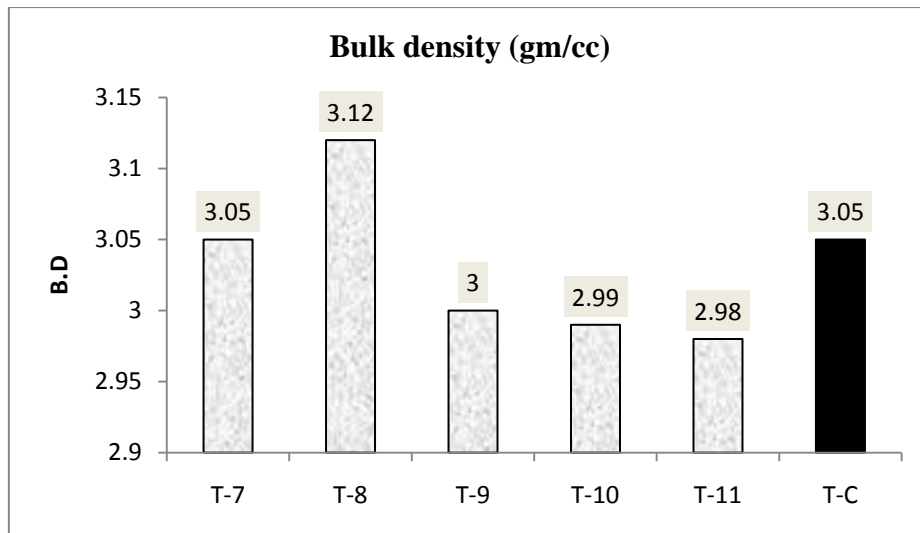


Fig.4.11: variation of bulk density with the increase of graphite content.

The variation of bulk density with the graphite content variation is shown in fig:4.11. It is seen that bulk density sharply increases from 3.05 gm/cc to 3.12 gm/cc with the increase of graphite content from 1 to 3 wt %. This may be due to the filling of voids by graphite particles. But at higher percentage of graphite bulk density decreases sharply from 3.05 gm/cc to 2.98 gm/cc for graphite content of 1 wt % to 9 wt% respectively. It is related to the lesser extent of higher percentage of graphite to the pores or voids, thus increases the overall volume of the sample. Also increase in graphite results in the decrease in dense MgO aggregate thus fall in BD. The BD of T-11 is much lesser than the conventional. This is due to larger volume of nano carbon present.

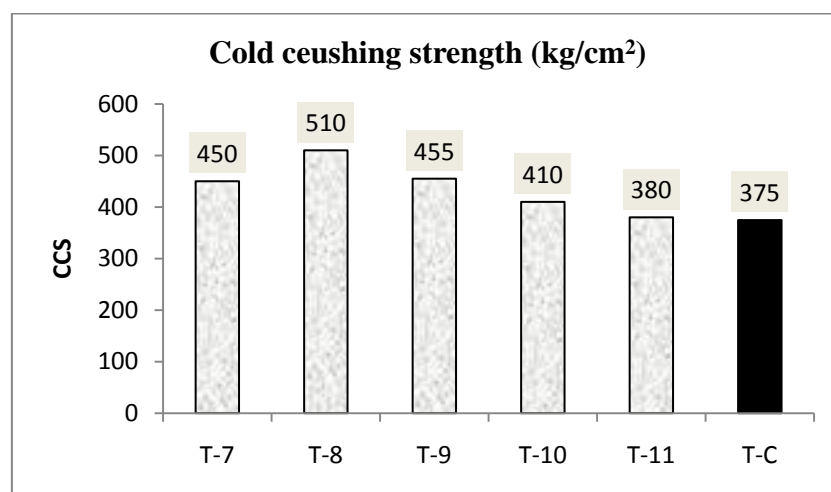


Fig.4.12: variation of cold crushing strength with the increase of graphite content.

The change in the values of cold crushing strength with the graphite content variation is shown in figure: 4.12. Initially the CCS values increases with the increase of graphite content and attains a maximum value of 510 kg/cm² for 3 wt% graphite as shown in T-8. This is because of, initially with the increase of graphite content increases the pore filling results in an increase in BD. But further increase of graphite content decreases the MgO aggregate phase. Also increase the volume due to the increase percentage of fine graphite content, resulting in decrease in strength. The 0.9 wt% nano carbon containing MgO-C with 3wt% graphite has much more CCS values has the conventional one.

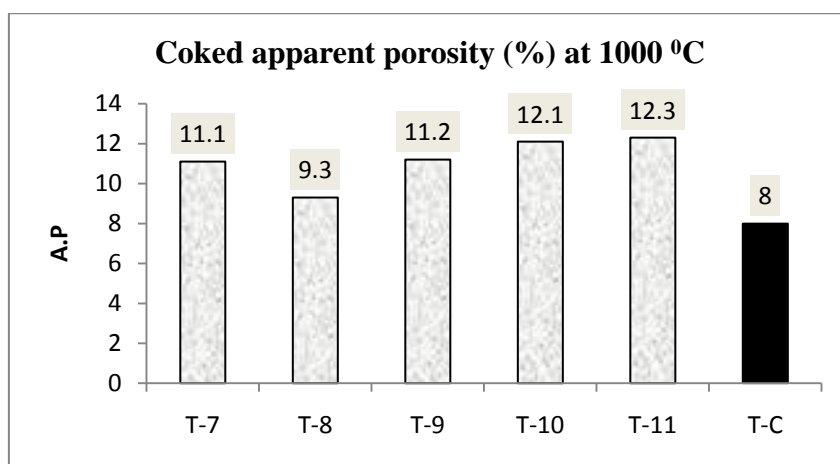


Fig.4.13: variation of coked apparent porosity crushing strength with the increase of graphite content.

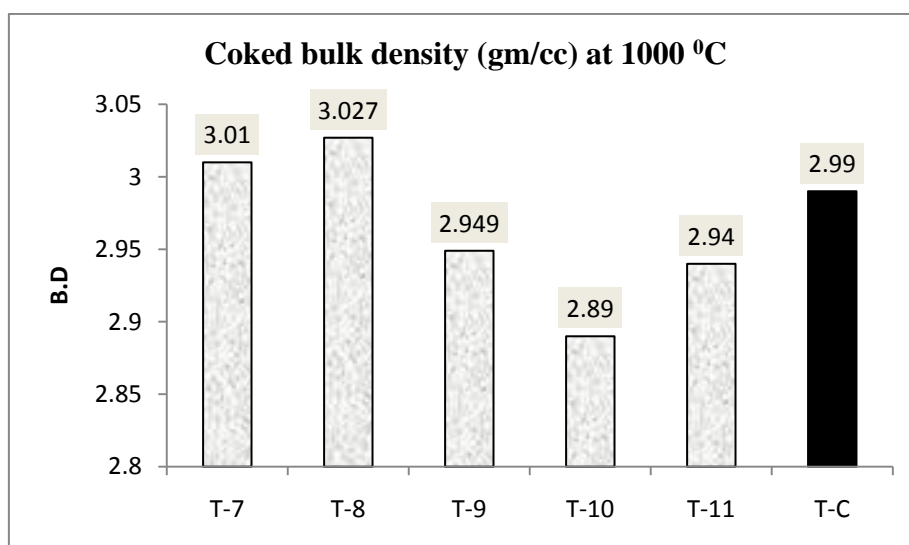


Fig.4.14: variation of coked bulk density with the increase of graphite content.

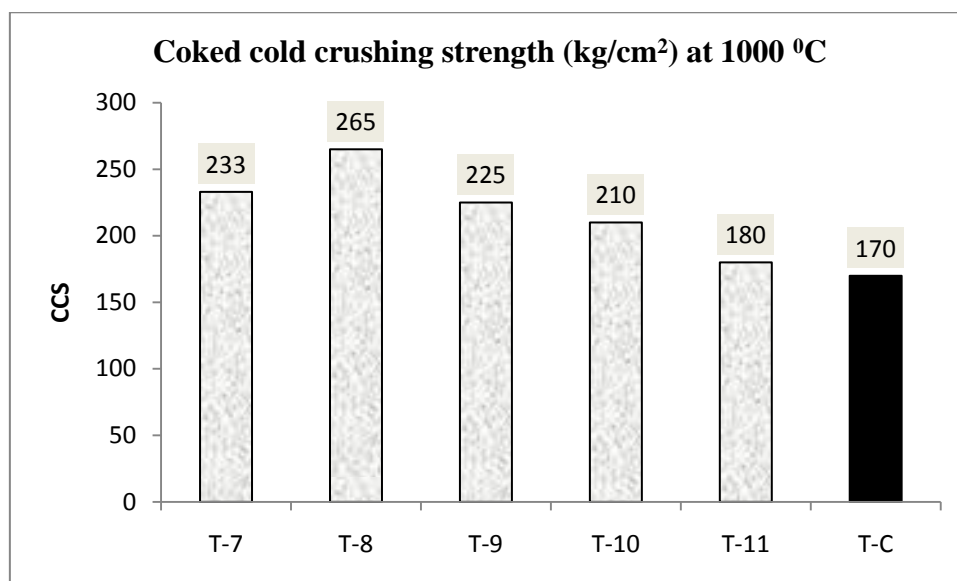


Fig.4.15: variation of coked cold crushing strength with the increase of graphite content.

The coked AP, BD and CCS values are shown in fig:4.13, fig:4.14 and fig:4.15 respectively. The coked AP, BD and CCS values ranges much lower than that of before coking. The coked AP, BD and CCS values are lowered because of the breaking of the interlocking texture that has been created after polymerization of phenolic resin.

4.3.2 Hot modulus of rupture:

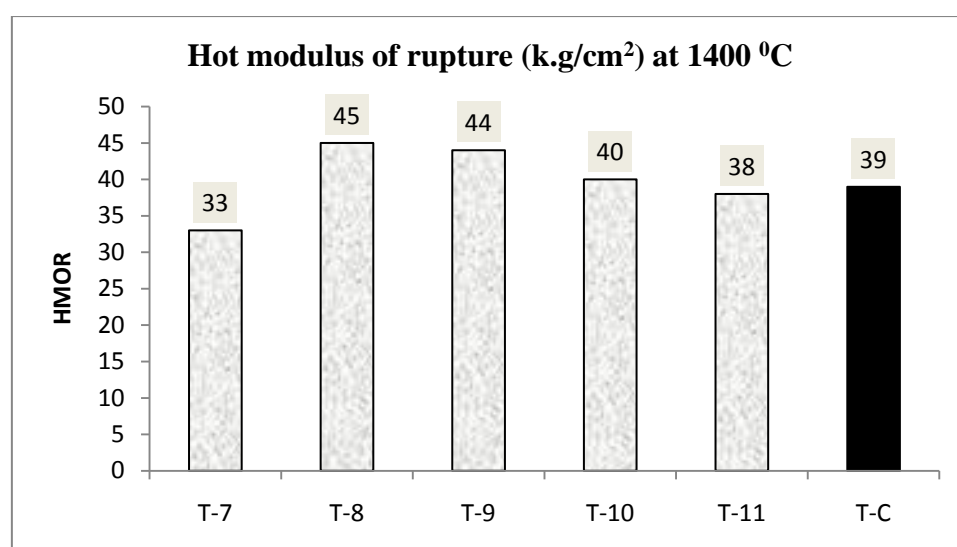


Fig.4.16: variation of hot modulus of rupture with the increase of graphite content.

The variation of HMOR with the variation of graphite content is shown in fig:4.16. The increase in graphite content increases the value of HMOR due to the increase of carbide formation. But further increases of graphite content filling of pores is less, graphite not entirely in aggregate structure but it also remain open .It increases the chances of oxidation .Though the chances of carbide formation increases but HMOR value decreases with the increase of graphite content because of the chances of higher oxidation.

4.3.3 Oxidation resistance:

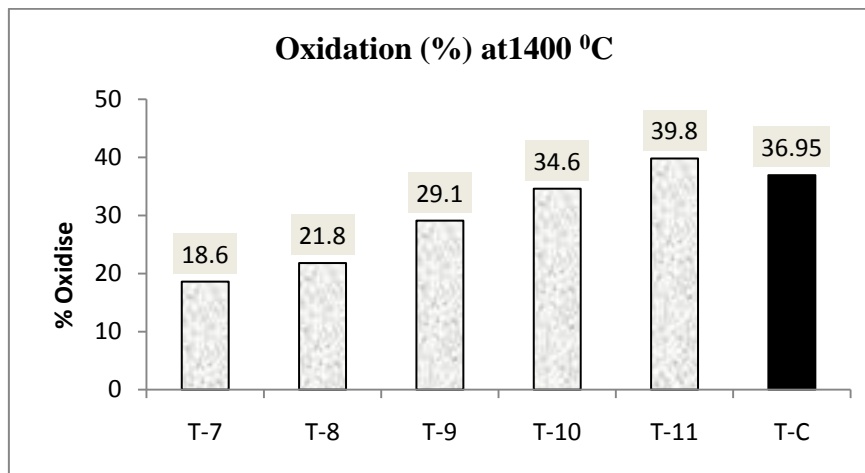


Fig.4.17: Variation of oxidation resistance with the increase of graphite content.

The change in oxidation resistance with the increase of graphite content is shown in fig:4.17. With the increase of graphite content the percentage of oxidation increases linearly, resulting in a poor oxidation resistance. There is a high change in oxidation percentage from 18.6% (T-7) for 1 wt% graphite to 39.8 % (T-11) for 9 wt% graphite content .It is due to the more graphite means more oxidation. Though the carbon content in T-11 and T-C are almost same but the oxidation percentage of T-11 is higher than that of T-C. This is due to the fact that T-11 contains nano carbon, which is much free and active, and gets oxidized faster.

4.3.4 Modulus of elasticity:

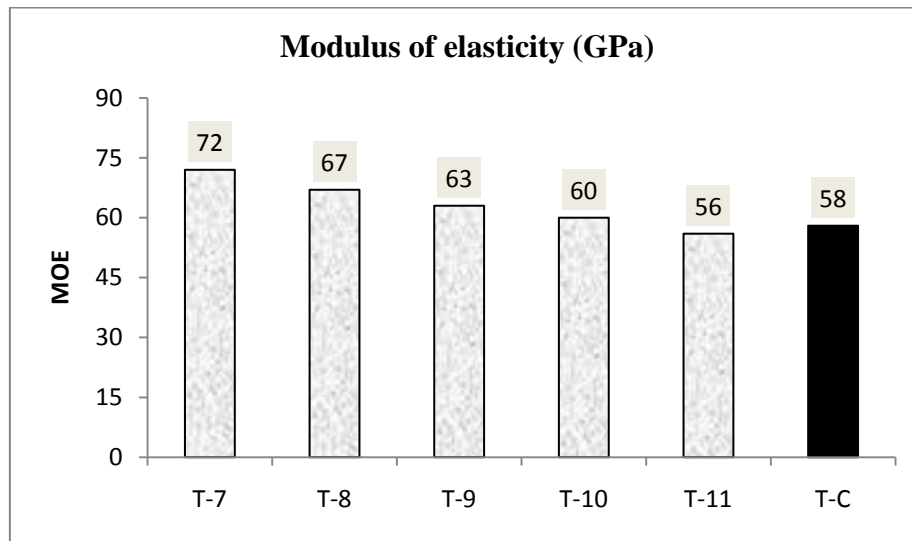


Fig.4.18: Variation of modulus of elasticity with the variation of nano carbon percentage.

Fig:4.18 describes the variation of MOE with the increase of graphite content for a fixed of 0.9 wt% nano carbon. In T-7 where there is only 1 wt% graphite and 0.9 wt% nano carbon and the MOE value is very high. With the increase of graphite content for a fixed of 0.9 wt% nano carbon the MOE values decrease linearly. T-11, containing 9 wt% graphite and 0.9 wt% nano carbon shows a lower value. The value of T-11 is similar to that of T-C containing 10 wt% graphite. Though the graphite content in T-11 is less than that of T-C but due to the presence of 0.9 wt% nano carbon the MOE value is lower.

4.3.5 Summary:

For batches T-7 to T-11, it was observed that for some properties T-9 containing 5 wt% graphite and 0.9 wt% nano carbon shows better result.

Also for some properties such as AP, Coked AP etc T-8 containing 3wt% graphite shows better result.

So for further study of suitable anti-oxidants and percentage of anti-oxidants both the batches T-8 and T-9 was taken as basic composition.

4.4 Physical and chemical properties of nano carbon added low carbon MgO-C bricks for 5wt% graphite and 0.9wt% nano carbon by varying the anti-oxidants percentage and compared with 10% graphite containing MgO-C brick:

4.4.1 Apparent porosity, Bulk density and Cold crushing strength (Before and after coking):

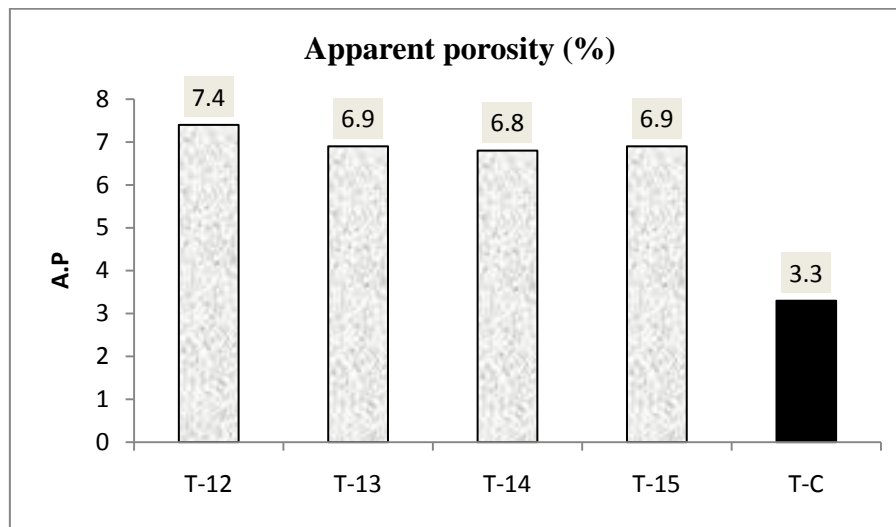


Fig.4.19: Change in apparent porosity with the variation of antioxidants.

Variation in apparent porosity with antioxidant variation is shown in fig:4.19. It is observed from figure that the variation in AP with the antioxidant variation is very less, mainly due to near similar composition and grain size distribution. The porosity of T-12 is 7.4%, after which it is almost constant to 6.9%.

However conventional products showed much less porosity level only 3.3%, may be due to the absence of nano carbon in the system. Nano carbon being very fine has very large volume and increases volume of the matrix phase and porosity.

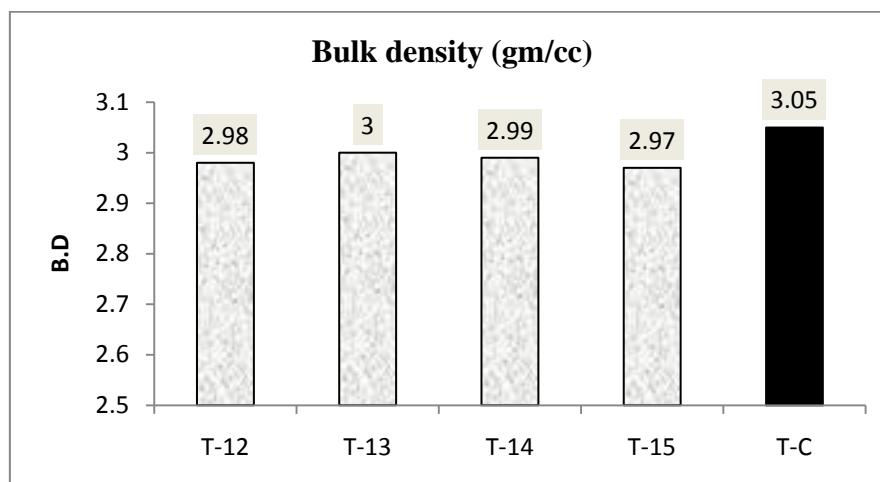


Fig.4.20: Change in bulk density with the variation of antioxidants.

Variation in bulk density with the antioxidants variations is shown in figure: 4.20. The variation is very less and is almost constant. The maximum variation is 0.03%. However the nano carbon containing bricks has much less value than the conventional one. This is due to the presence of nano carbon. Nano carbons have very fine size and large volume, thus results in a decrease in bulk density.

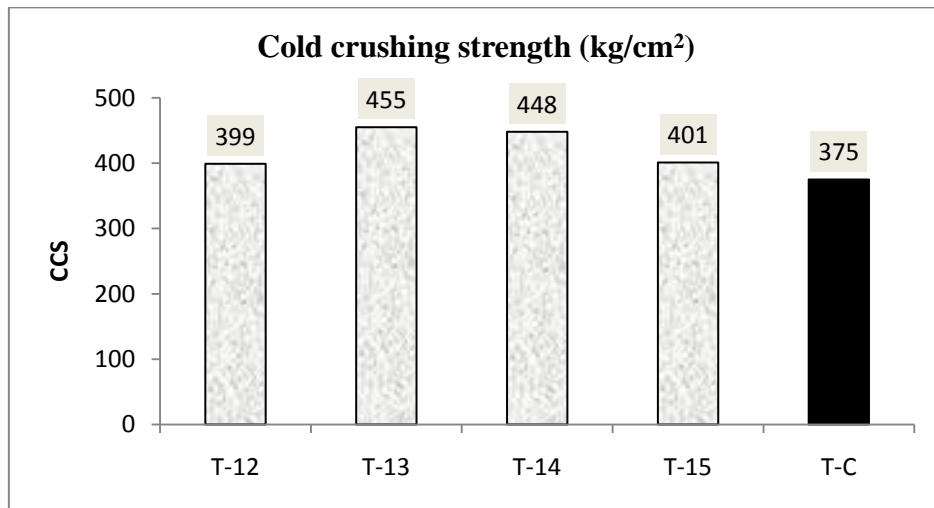


Fig.4.21: Change in cold crushing strength with the variation of antioxidants.

Fig: 4.21 describe the variation of cold crushing strength with the variation of antioxidants. There is not much differences in CCS among different batches. However nano carbon containing ones shows marginally increase in CCS. The presence of nano carbon increases the filling activity of inter-granular pores hence the strength increases compared to the without nano carbon conventional batch.

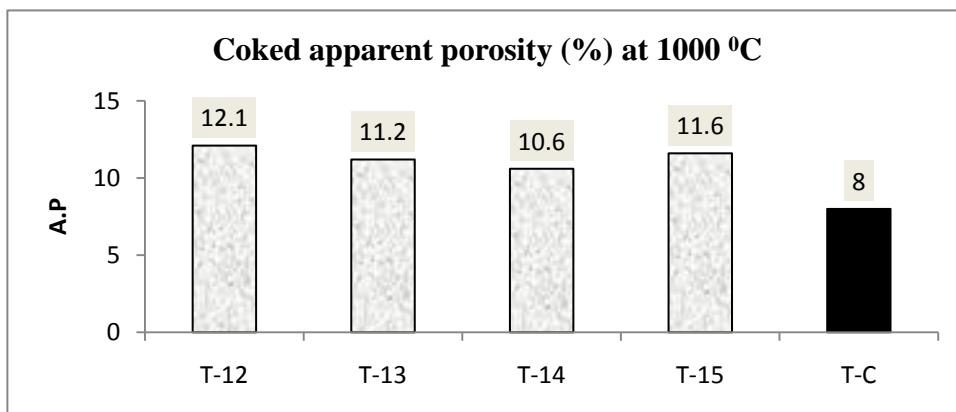


Fig.4.22: Change in coked apparent porosity with the variation of antioxidants.

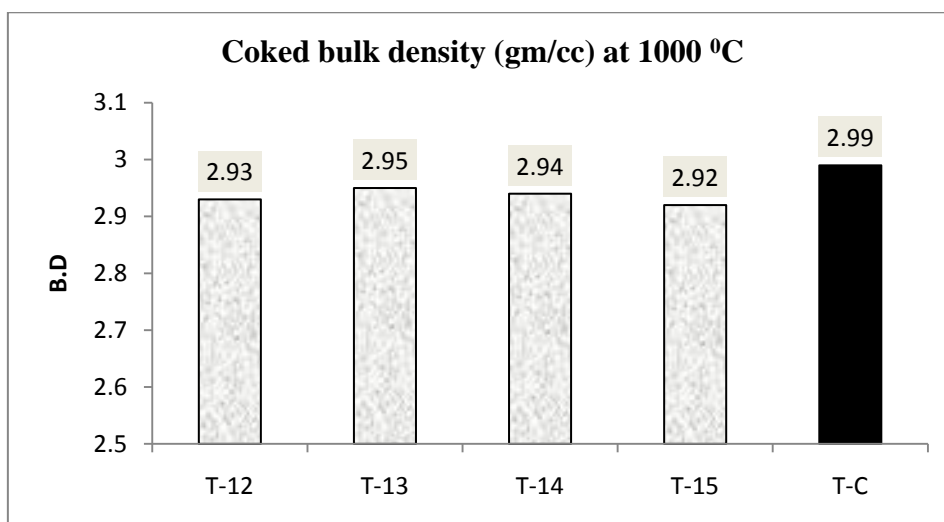


Fig.4.23: Change in coked bulk density with the variation of antioxidants.

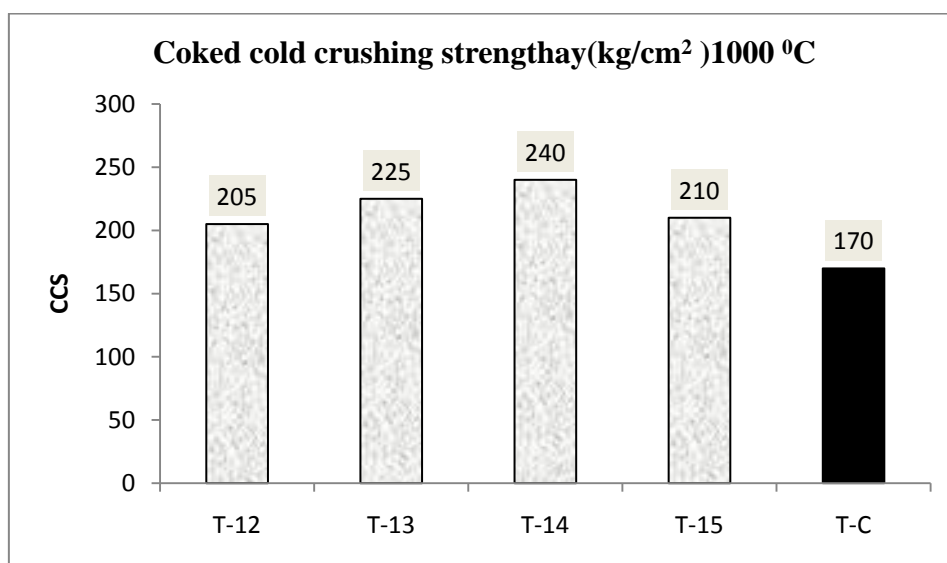


Fig.4.24: Change in coked cold crushing strength with the variation of antioxidants.

The coked AP, BD and CCS values are shown in fig:4. 22, fig:4.23 and fig:4.24 respectively. The coked AP, BD and CCS values changes almost in the same fashion as that of before coking. The breaking of the interlocking texture was due to the burning out of the total organic portion of resin and release of harmful decomposition gases such as benzene, toluene, phenols and xylene, results in decrease of AP, BD and CCS values after coking.

4.4.2 Oxidation resistance:

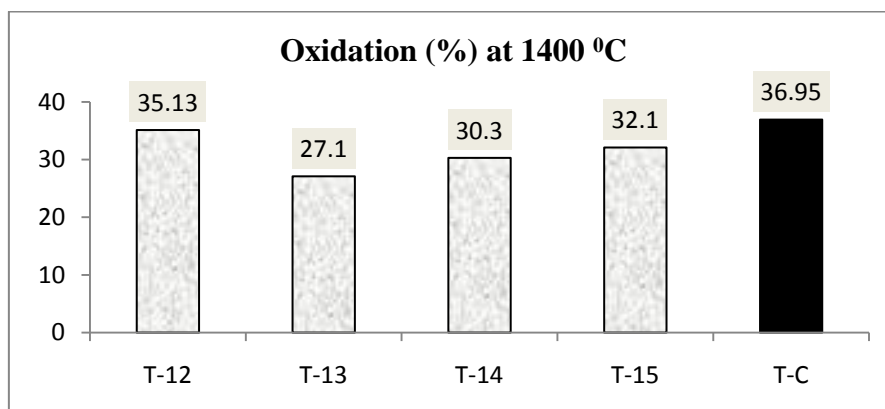
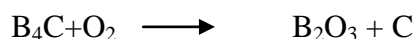


Fig.4.25: Change in oxidation resistance with the variation of antioxidants.

The change in oxidation resistance with different antioxidants is shown in fig: 4.25. Without nano carbon containing conventional batches show maximum oxidation. As no antioxidant is there in T-12, graphite and nano carbon are exposed to oxygen and oxidizes. The value is lesser than T-C batch. T-C shows higher oxidation may be due to the higher amount of graphite presence in the batch (10 wt%) compared to other batches (graphite 5 wt% and nano carbon 0.9 wt%). T-13 containing 0.5 wt% Al and 0.5 wt% B₄C showed highest oxidation resistance. B₄C the best antioxidant for nano carbon at lower temperature improves the oxidation resistance.



This reaction occurs at lower temperature thus preventing oxygen to react with nano carbon, whereas Al acts better at relatively higher temperature. Nano carbon starts oxidise at low temperature due to the high fineness and reactivity. So B₄C is essential to prevent the same. Lowering in B₄C content reduces oxidation resistance as seen from batch T-14 and T-15.

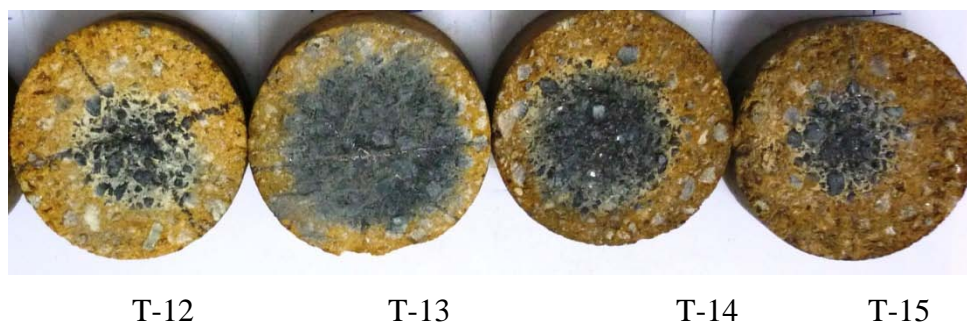


Fig.4.26: Oxidation samples after cutting.

4.4.3 Hot modulus of rupture:

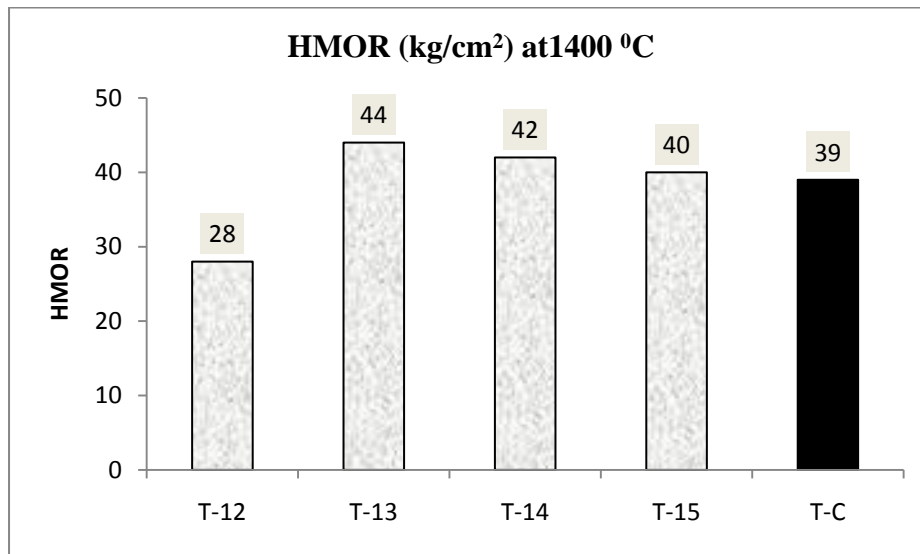


Fig.4.27: Change in hot modulus of rupture with the variation of antioxidants.

Fig: 4.27 shows the change in HMOR with the different antioxidants. Without antioxidant containing T-12 shows minimum HMOR values as the carbon in matrix gets oxidized, resulting porous structure, gives minimum HMOR. Presence of antioxidants provides much increase in HMOR values for all the batches. T-13 containing 0.5 wt% Al and 0.5 wt% B₄C shows highest HMOR as B₄C prevents oxidations even from low temperature, and Al reacts to form carbides thus increases the strength (HMOR). Decrease in B₄C content have higher oxidation and resulting relatively porous structure in matrix and little fall in HMOR as found in T-14 and T-15. T-C batch without any nano carbon and B₄C shows similar values as T-15. Al alone can act as good antioxidant however higher extent of carbon as graphite increases oxidation, results porous structure. So HMOR is not higher though the carbide formation is there.

4.4.4 Modulus of elasticity:

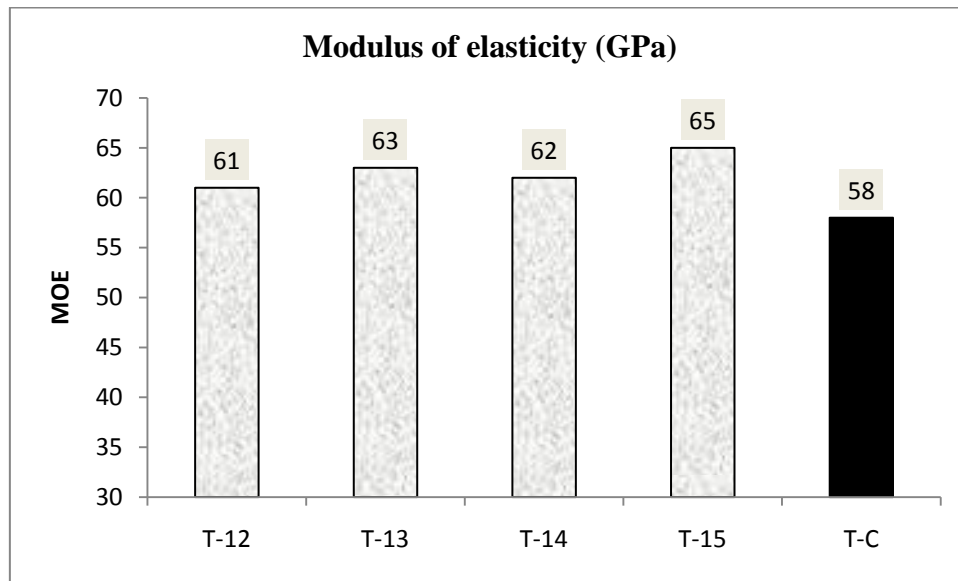


Fig.4.28: Variation of modulus of elasticity with the variation of anti-oxidants.

Fig: 4.28 shows the variation of modulus of elasticity with the variation of anti- oxidants for 5 wt% graphite and 0.9 wt% of nano carbon of each batch. There is no much variation of MOE values with the variation of anti-oxidants. Because there is no role of anti-oxidants on the MOE values. Due to the similar composition the filling is almost same and the MOE values are almost similar. In general the nano carbon containing batches have the higher values than the conventional MgO C composition.

4.4.5 Summary:

The effect of B_4C is observed. With the increase of B_4C content both the oxidation resistance and HMOR values improved. T-13 containing 0.5 wt% of Al and 0.5 wt% of B_4C as anti-oxidants shows better result.

4.5 Physical and chemical properties of nano carbon added low carbon MgO-C bricks for 3wt% graphite and 0.9wt% nano carbon and varying anti-oxidants percentage and compared with 10% graphite containing MgO-C brick:

4.5.1 Apparent porosity, Bulk density and Cold crushing strength (Before and after coking):

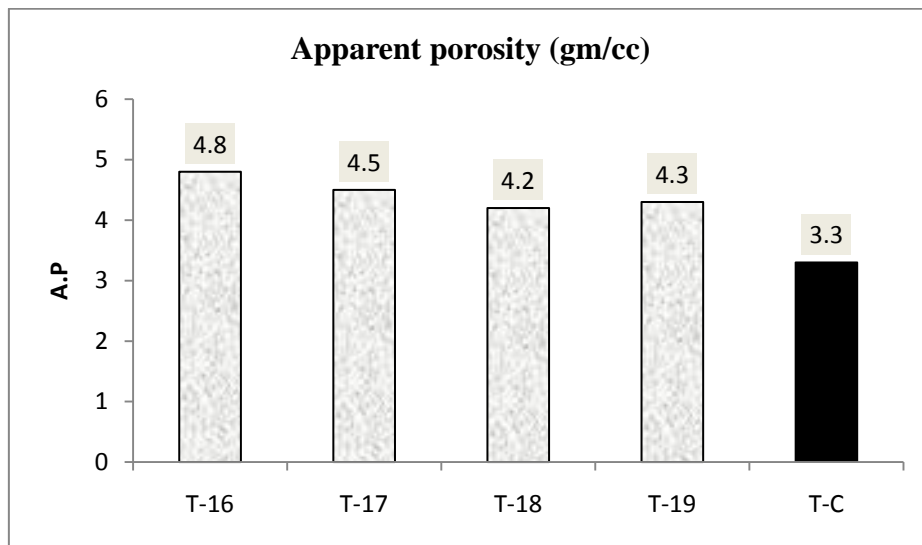


Fig.4.29: Change in apparent porosity with the variation of antioxidants for 3 wt% graphite.

The variation of apparent porosity with the different antioxidants with 3 wt% graphite is shown in fig: 4.29. From T-16 to T-18 the nano carbon contains 0.9 wt%. Presence in nano carbon gives the better filling between different refractory particles. T-C containing 10 wt% graphite has the better filling, results in lower AP. The variation in anti-oxidants does not have much effect on the AP values because the particle size distribution remains almost same. However T-16 has the highest AP whereas T-18 has the lower one.

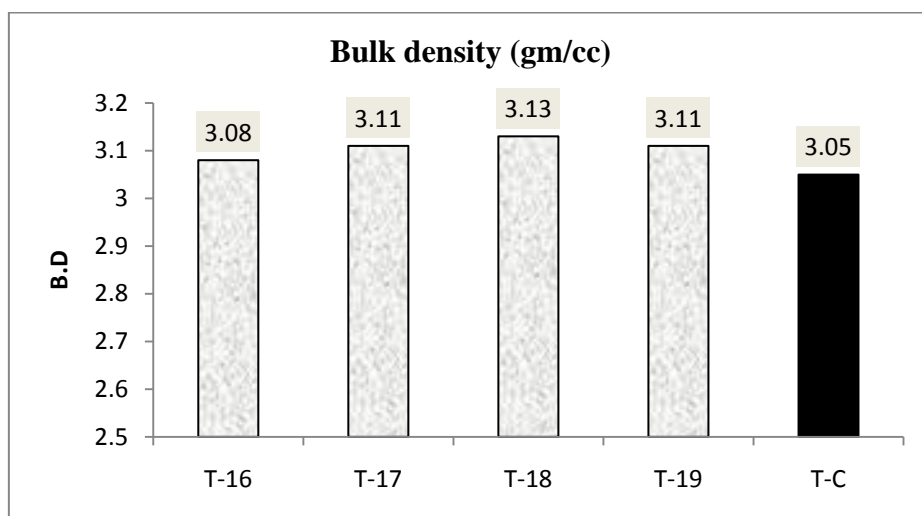


Fig.4.30: Change in bulk density with the variation of antioxidants with 3 wt% graphite

Fig: 4.30 explains the variation of bulk density with the variation of antioxidants with 3 wt% graphite. The filling with nano carbon increases the bulk density. Though the variation in bulk density is very less. T-C has better filling as graphite content is higher (10 wt%) but decreases the MgO wt% in the aggregate. MgO having the high density, so decrease in MgO content decreases the bulk density of T-C. This is why the nano carbon containing batches have higher BD than that of T-C.

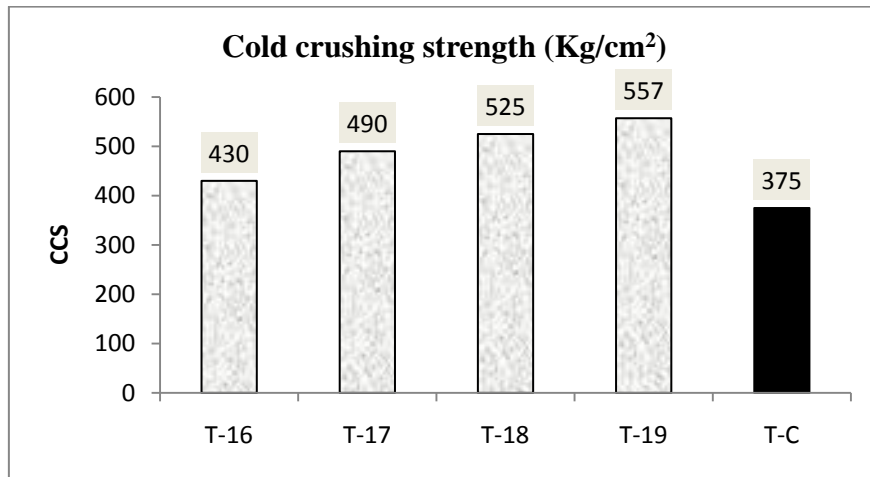


Fig.4.31: Change in cold crushing strength with the variation of antioxidants with 3 wt% graphite.

Fig: 4.31 describes the variation in cold crushing strength with the variation of antioxidants with 3 wt% graphite. The CCS values increases linearly from T-16 to T-19. Due to the better filling, lower in AP values and higher the BD promotes the higher CCS values. For T-C higher filling is done but higher graphite content increases the volume of the matrix decreases the CCS value.

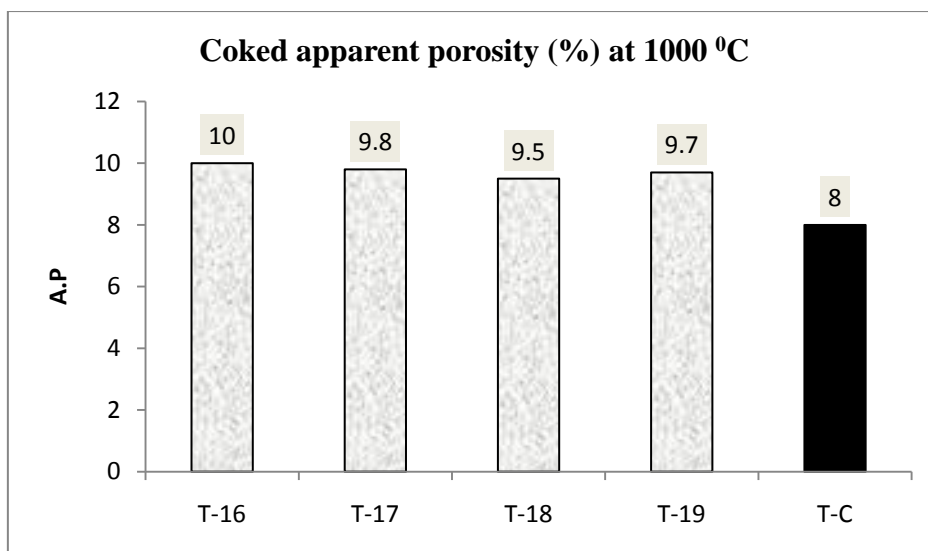


Fig.4.32: Change in coked apparent porosity with the variation of antioxidants with 3 wt% graphite.

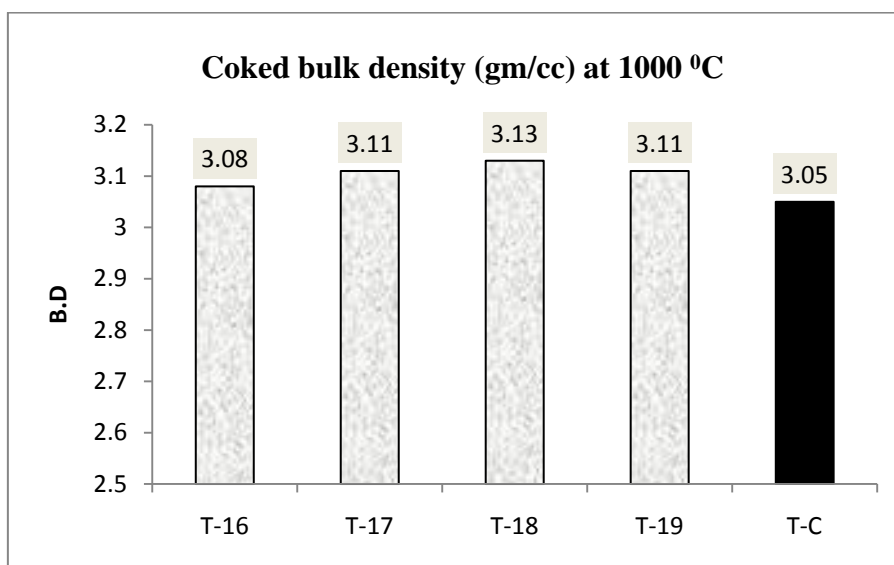


Fig.4.33: Change in coked bulk density with the variation of antioxidants with 3 wt% graphite.

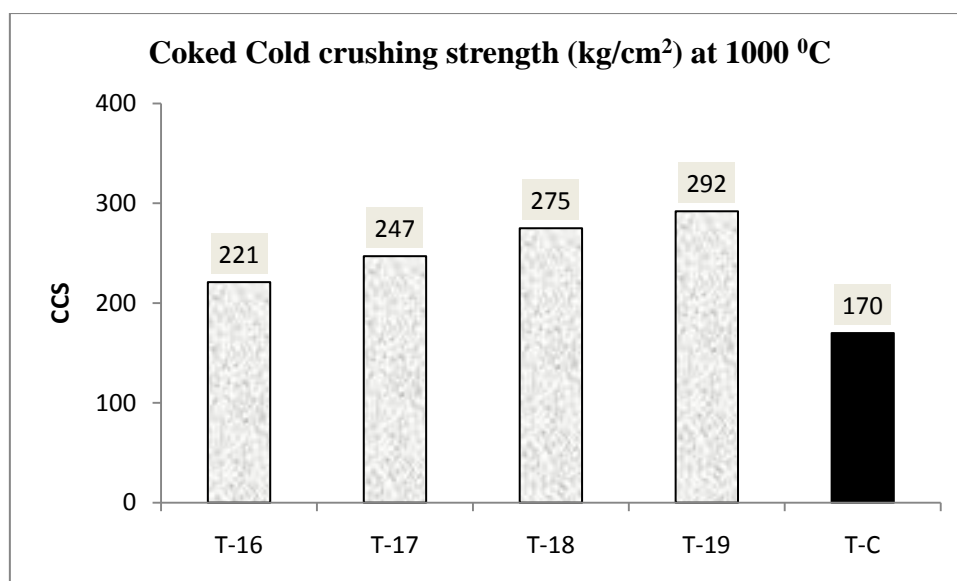


Fig.4.34: Change in coked cold crushing strength with the variation of antioxidants with 3 wt% graphite.

The coked AP, BD and CCS values are shown in fig: 4.32, fig: 4.33 and fig:4. 34 respectively. The coked AP, BD and CCS values are much lower than that of before coking. The coked AP, BD and CCS values are lowered because of the breaking of the interlocking texture that has been created after polymerization of phenolic resin.

4.5.2 Hot modulus of rupture:

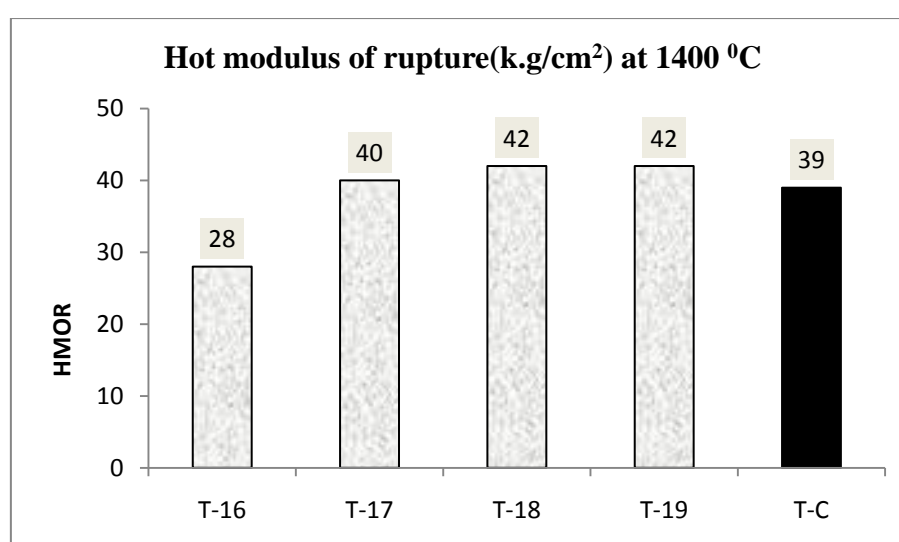


Fig.4.35: Change in hot modulus of rupture with the variation of antioxidants with 3 wt% graphite

HMOR values of 3 wt% graphite containing with various antioxidants can be explained with fig: 4.35. T-16 has lower HMOR values whereas T-18 and T-19 have higher HMOR values. This is because T-16 contains no anti-oxidants and T-17 contains 0.5wt% of Al powder and 0.5 wt% of B₄C. As anti-oxidant content increases, improves the oxidation resistance thus improving the HMOR values.

4.5.3 Oxidation resistance:

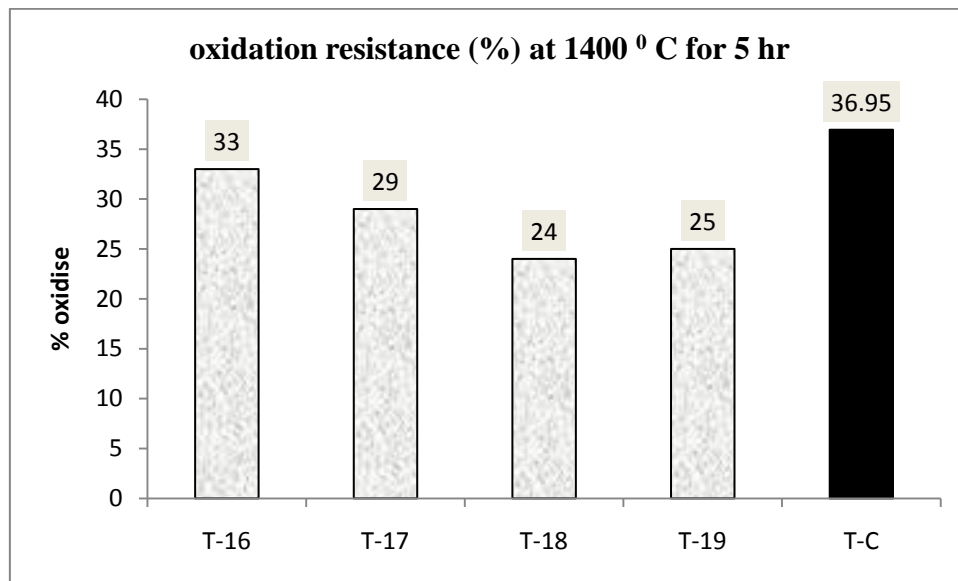


Fig.4.36: Change in oxidation resistance with the variation of antioxidants with 3 wt% graphite.

The change in oxidation resistance with 3 wt% graphite and different antioxidants are shown in fig: 4.36. T-16 doesn't contain any anti-oxidant thus it showed maximum oxidation. T-17 contain 0.5 wt% Al powder and 0.5 wt% B₄C. As the anti-oxidant content increase, improve the oxidation resistance. With the increase in B₄C content, the oxidation resistance improved, as observed for T-18 and T-19.

4.5.4 Modulus of elasticity:

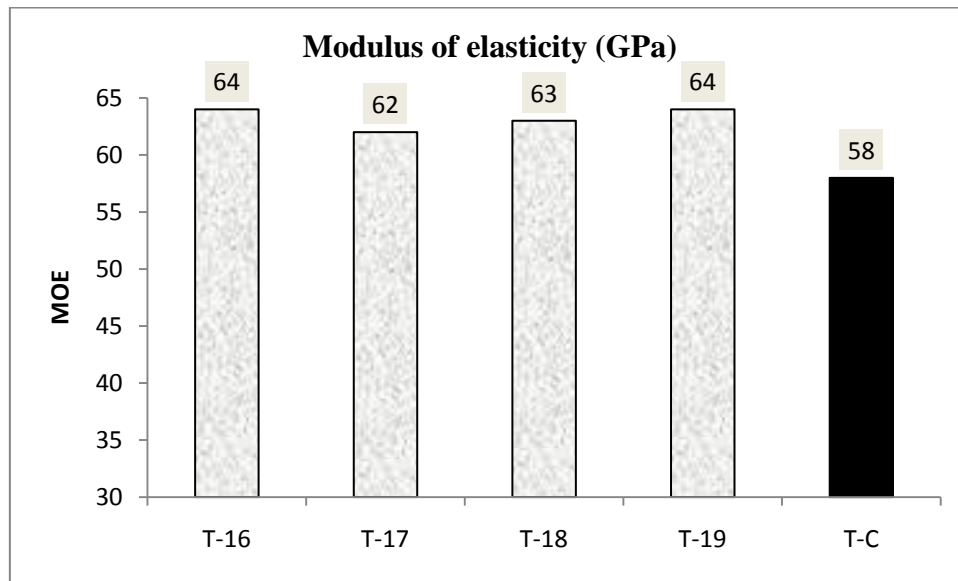


Fig.4.37: Variation of modulus of elasticity with the variation of anti-oxidants.

Fig: 37 shows the variation of MOE values with the variation of anti –oxidants for containing 3 wt% graphite and 0.9 wt% nano carbon for all batches. There is not much variation of MOE values with the variation of anti-oxidant, because there is no role of anti-oxidants on the MOE values. Due to the similar composition the filling is almost same and the MOE values are almost similar. The nano carbon containing batches have the higher values than the 10 wt% graphite containing T-C batch.

4.5.5 Summary:

T-18 containing 0.8 wt % Al and 0.2 wt% B₄C shows better result.

Some properties such as AP, Coak AP, oxidation etc. shows better result than 5wt% graphite containing batches.

4.6 Some properties of nano carbon added low carbon MgO-C bricks compared with the 10% graphite containing MgO-C brick:

4.6.1 Corrosion resistance:

Static crucible slag corrosion:

Fig.4.38 shows the cross section of the refractory containing without and with nano carbon after slag corrosion test. Incorporation of nano carbon dramatically inhibits the slag corrosion

and penetration resistance followed by without and different wt%.carbon, having the high contact angle is non- wetting in nature. So it improves the corrosion resistance. The effect of carbon is more prominent when the particle size of carbon decreases to nano level as the reactivity, surface area, and surface volume increases by many folds. Nano carbon being very fine in nature possess high reactivity, high surface area and specific volume thereby forming a coating on the surface of graphite leading to prevention of decarburization of graphite from the matrix[82,131] .Hence addition of 0.3 wt%,0.6 wt% and 0.9 wt% nano carbon in MgO-C refractory exhibits higher oxidation resistance thereby leading to better slag corrosion and penetration resistance.

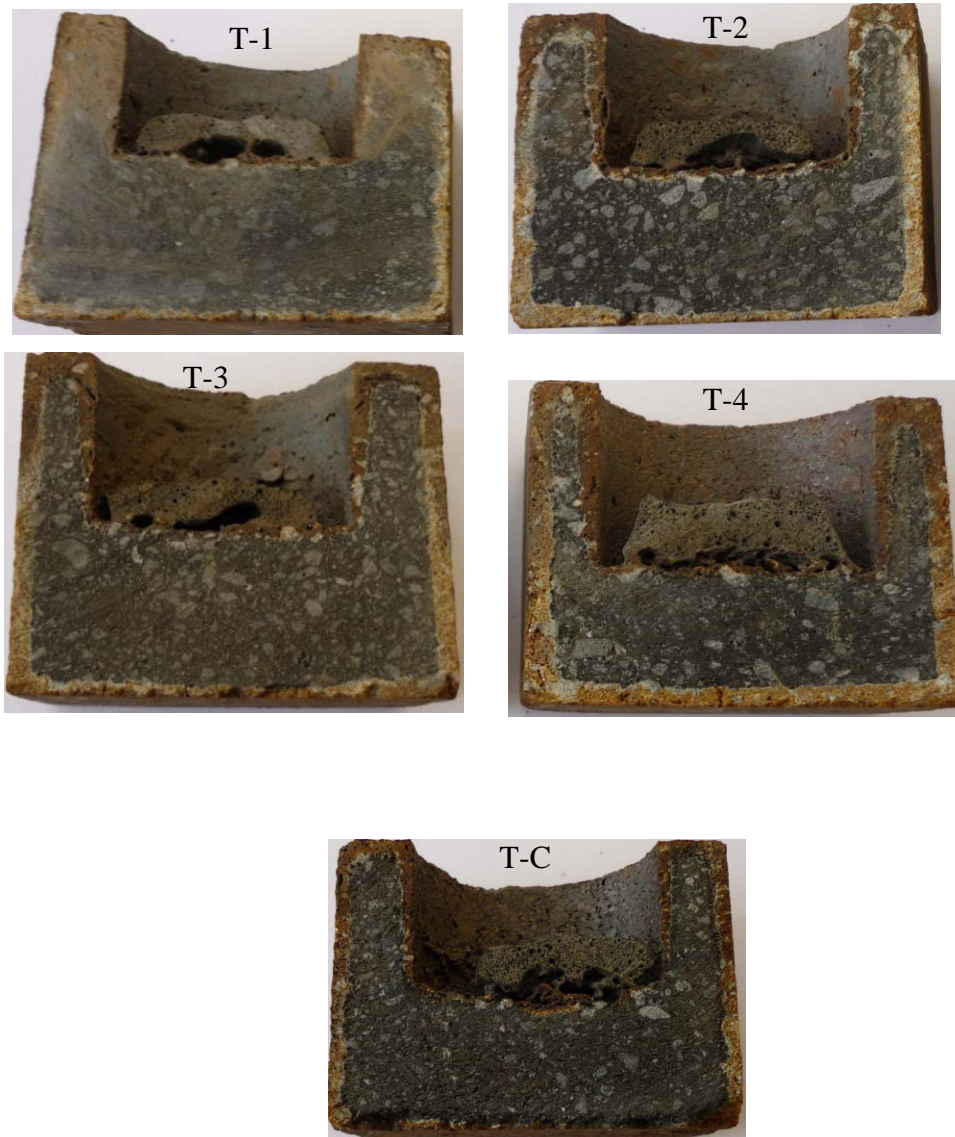


Fig.4.38: Corroded samples after cutting.

Fig.4.39 shows corrosion (mm) as a function of different nano carbon added MgO-C refractories. It is clearly indicated that the nano carbon added bricks undergone lowest

corrosion. The penetration depth is lowering with the increase of nano carbon percentage. Though the graphite percentage of T-1,T-2,T-3 and T-4 are same but penetration depth decreases with the increase of nano carbon percentage, because, the increase of nano carbon increases the distribution of carbon throughout the matrix. Thus, though in batch T-4 has only 3% graphite and 0.9% nano carbon it shows equivalent slag penetration resistance to that of T-C containing 10% graphite .Thus by adding nano carbon the slag corrosion resistance improves.

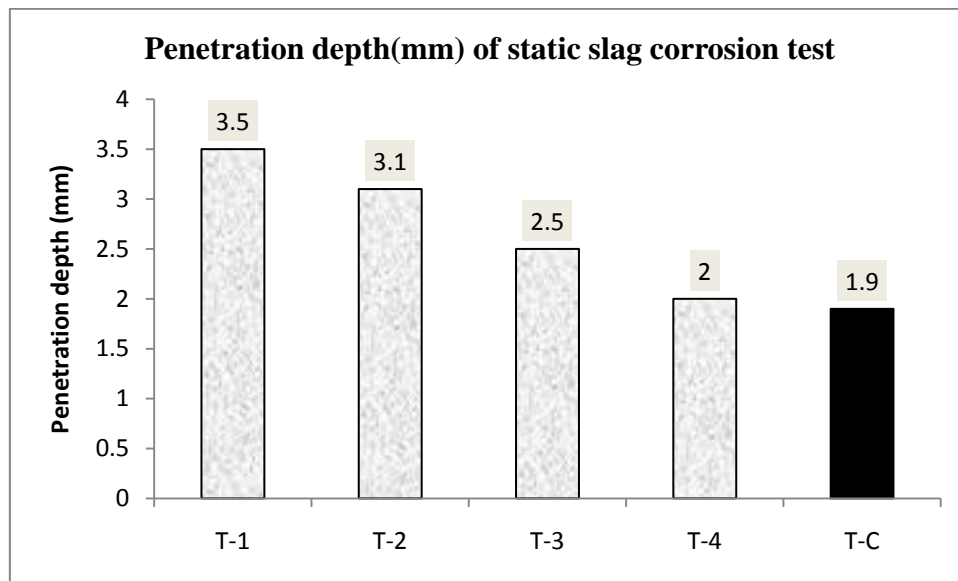


Fig.4.39: Graph of penetration depth of Static corrosion test.

4.6.2 Thermal Shock resistance:

The thermal shock resistance of different samples is shown in fig. T-1 containing 3 wt% graphite only shows lower thermal shock resistance. T-2 ,T-3 and T-4 containing 3 wt % graphite and nano carbon 0.3wt%,0.6wt% and 0.9 wt% respectively. As nano carbon percentage increases so distribution of carbon into the entire matrix increases, results in a better thermal shock resistance. This is due to the high surface area and high volume of nano carbon. T-C containing 10 wt% graphite shows a good thermal shock resistance .With the increase of graphite content the thermal conductivity of the brick increases, results in a good thermal shock resistance. It was observed that thermal shock resistance of T-C is double than that of T-1.

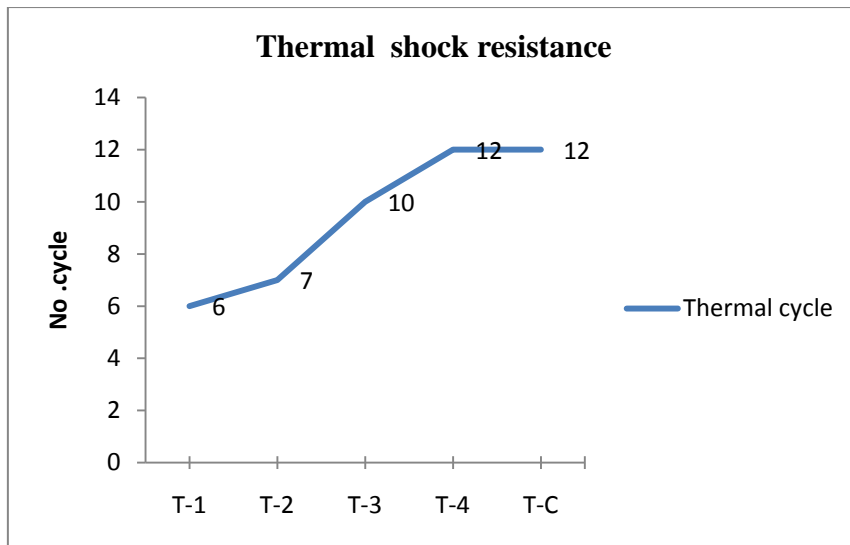


Fig.4.40: Graph of thermal shock resistance.



Fig.4.41: samples after 4th cycle.



Fig.4.42: Samples after 10th cycle.

4.6.3 Microstructure:

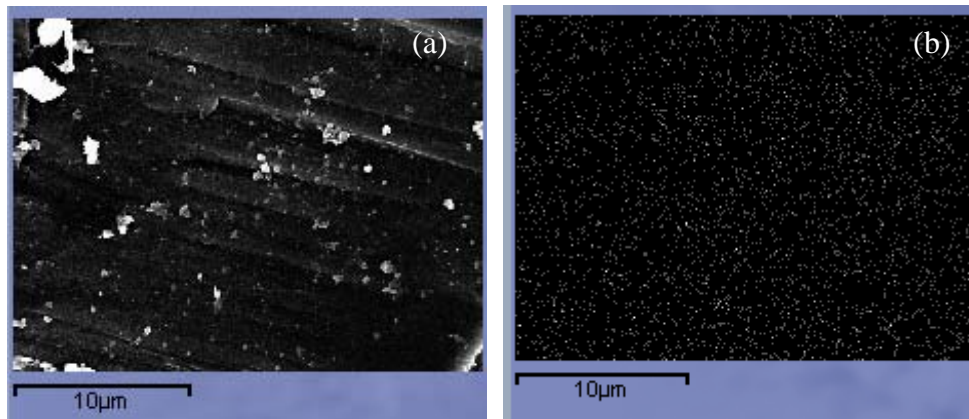


Fig.4.43(a)SEM picture of 3 wt% graphite and 0.3% nano carbon containing low carbon MgO-C brick (b) It's carbon mapping.

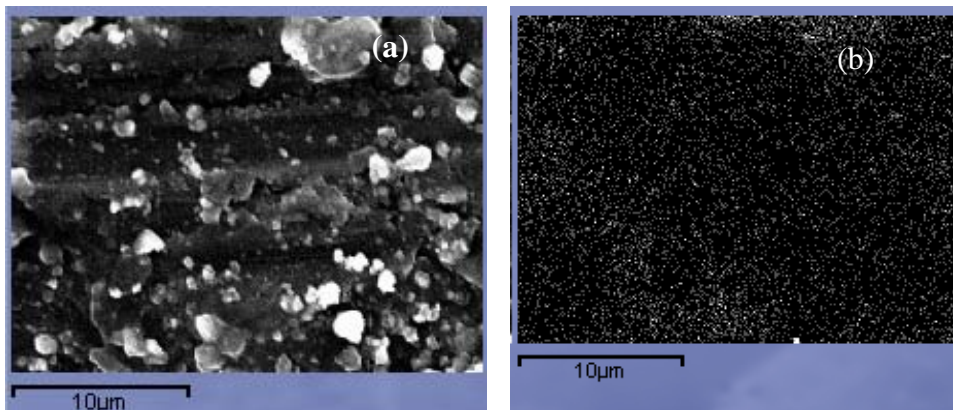


Fig.4.44:(a)SEM picture of 3wt% graphite and 0.9 wt% nano carbon containing low carbon MgO-C (b)It's carbon mapping

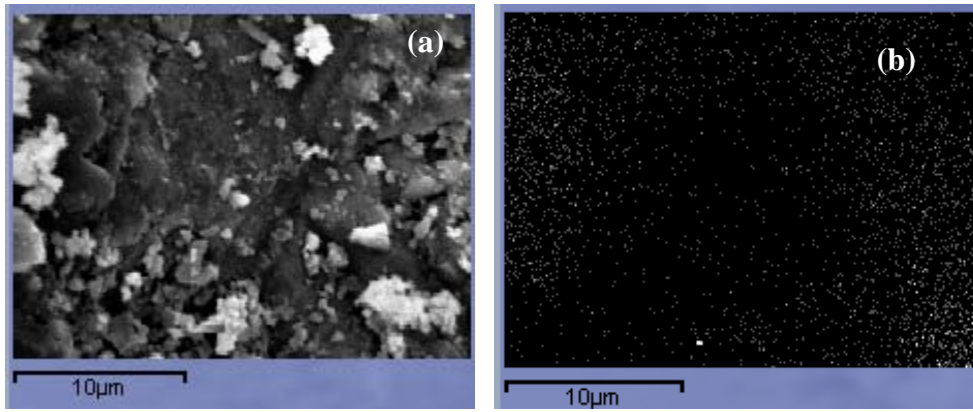


Fig.4.45:(a)SEM picture of 3wt% graphite and 0.9 wt% nano carbon containing low carbon MgO-C (b)It's carbon mapping

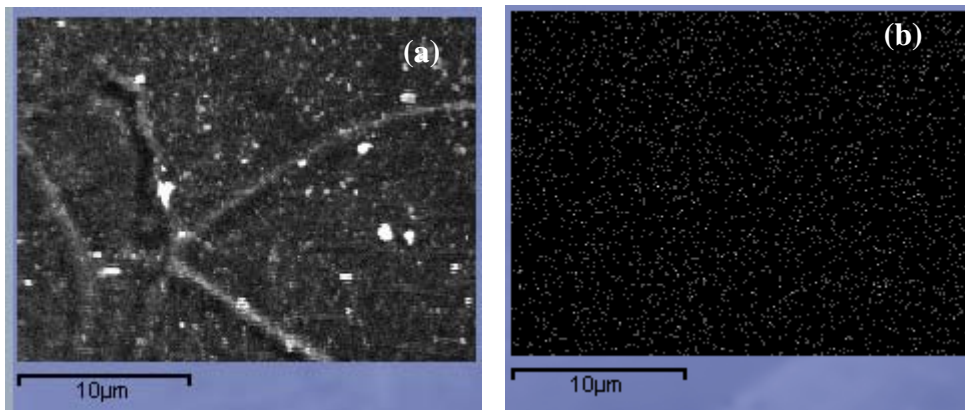


Fig4.46: (a) SEM picture of 10 wt% graphite containing MgO-C brick.(b) It's mapping.

These are the microstructure of 10 wt% graphite containing MgO-C brick as well as 3 wt% graphite and 0.3wt%,0.6wt% and 0.9wt% nano carbon containing low carbon MgO-C brick respectively. Here it was tried to observe the distribution of carbon in different samples. So the mapping of carbon was done of five points of each sample. It is clearly observed that fig 10 wt% graphite containing samples have almost uniform distribution of carbon. The distribution of carbon of 3wt% graphite and 0.3 wt% nano carbon containing samples of fig:43 is not so uniform. It is due to the less amount of graphite as well as nano carbon. Fig: containing 3 wt% graphite and 0.6 wt% nano carbon showed a very uniform distribution and it is almost similar to that of 10 wt% graphite containing samples. But with the increase of nano carbon percentage the chances of agglomeration of nano carbon increases. Because of the tendency of agglomeration of nano carbon the nano carbon are deposited at different

points .It is also observed in fig: 45, samples containing 3 wt% graphite and 0.9wt% nano carbon

4.6.4 Pore size distribution:

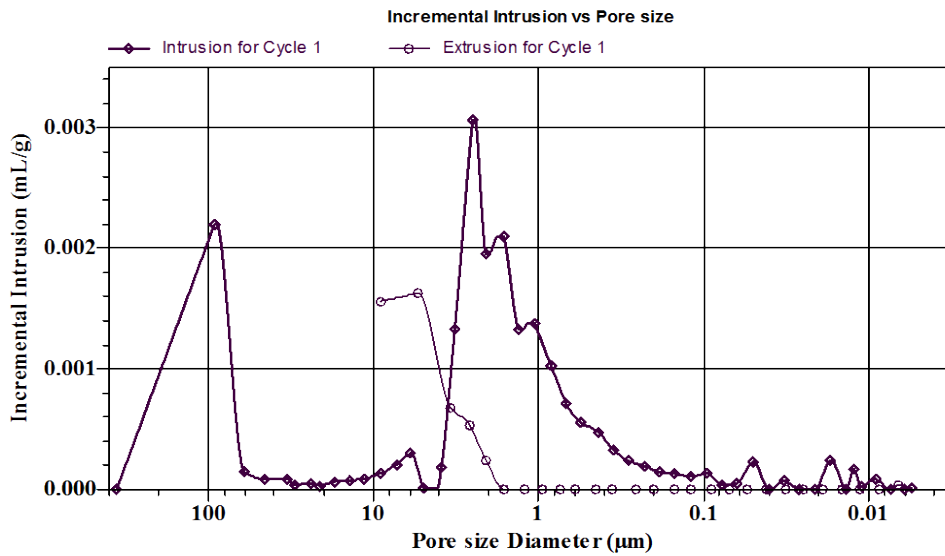


Fig.4.47: Incremental intrusion Vs pore size of sample with 3wt% graphite 0.3% nano carbon.

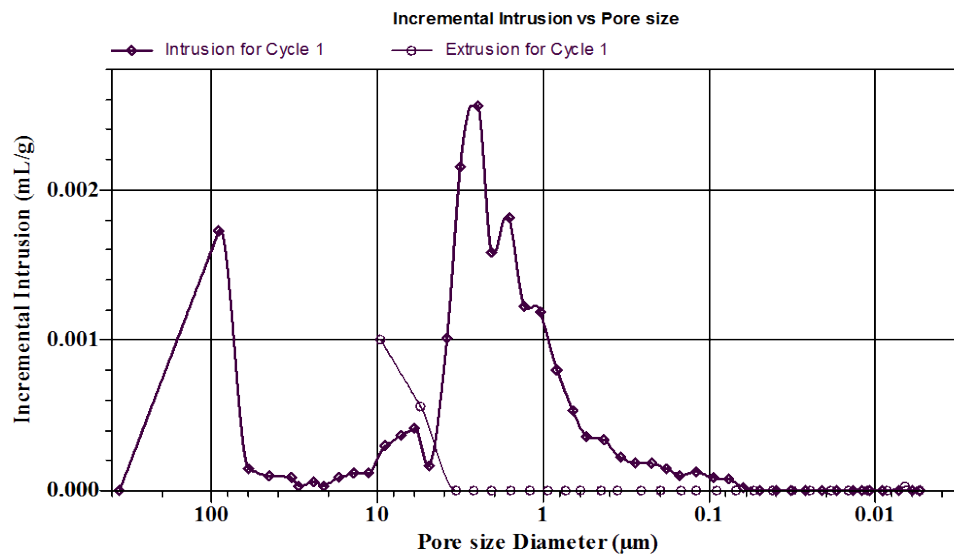


Fig.4.48: Incremental intrusion Vs pore size of sample with 3wt% graphite 0.6% nano carbon

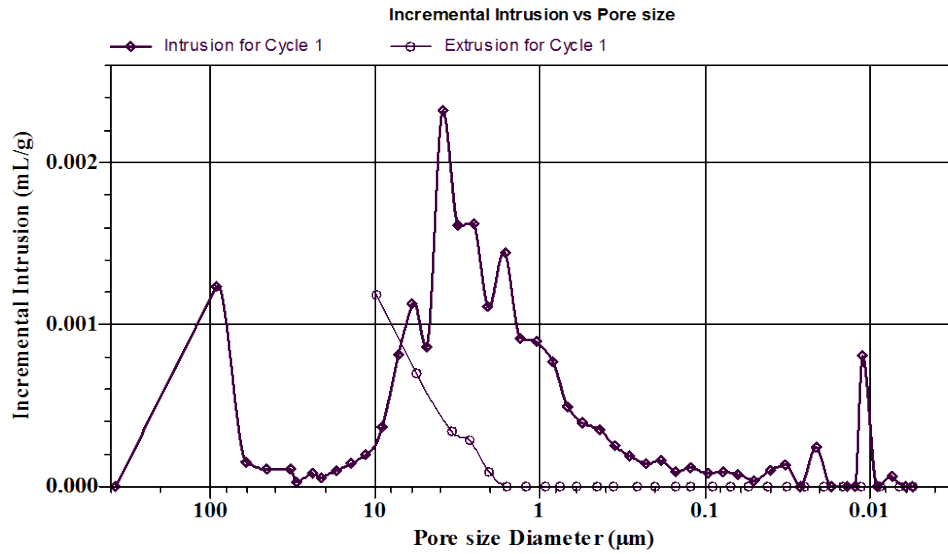


Fig.4.49: Incremental intrusion Vs pore size of sample with 3wt% graphite 0.9% nano carbon.

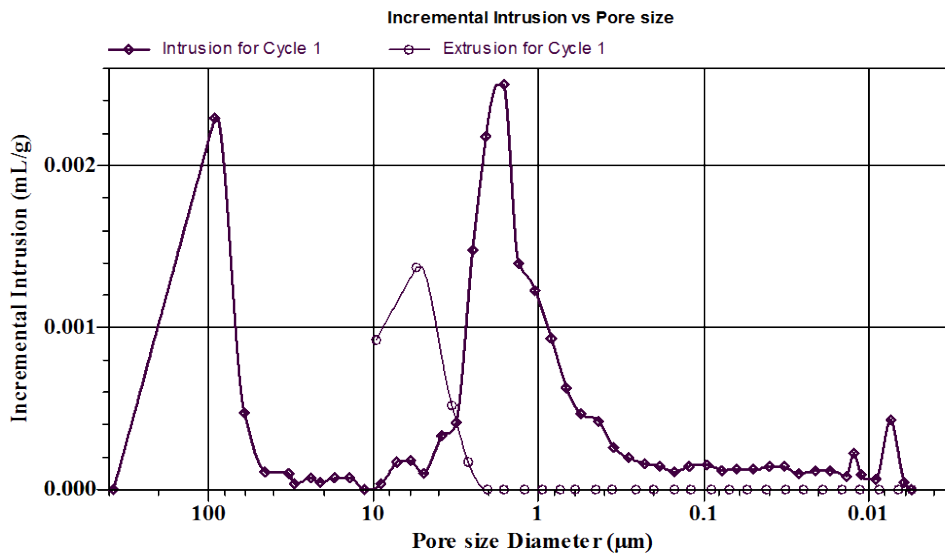


Fig.4.50: Incremental intrusion Vs pore size of sample with 10% graphite

It is observed that with the increase of nano carbon content the macro pores volume decreases. The incremental intrusion decreases with the increase of nano carbon content. It is due to the fill up of the spaces between different macro refractory particles by the nano carbon. The pore size diameter also decreases with the increase of nano carbon percentage. The 3 wt% graphite and 0.9 wt % added fig.4.49 has the minimum value of incremental intrusion and it is also better than the 10 wt% graphite containing MgO- C bricks.

4.6.5 Summary:

- The corrosion resistance of 3wt% graphite and 0.9 wt% nano carbon containing batches are almost similar to that of 10 wt% graphite containing batches.
- Thermal shock resistance of 3wt% graphite and 0.9 wt% nano carbon containing batches are also similar to that of 10 wt% graphite containing batches.
- The distribution of carbon in 3 wt% graphite and 0.6 wt% nano carbon containing batches are similar to that of 10 wt% graphite containing batches. With the increase of nano carbon greater than 0.6 wt% agglomeration occurs, which is confirmed through the carbon mapping of SEM pictures of nano carbon containing batches.
- By adding nano carbon the micro pores volume decreases.

Chapter-5

CONCLUSION

CONCLUSION:

Magnesia carbon bricks are becoming an essential lining material for the different zones of steel teeming ladles due to many advantages compared to the conventional alumina brick lining or alumina / alumina spinel castable linings. Now use of carbon in refractory has many advantages but as the eco-friendliness is becoming a great point in all aspect of steel manufacturing, use of carbon has started many negative aspects too. So globally the research trend is to minimize the carbon content in the refractories for better performances and lining life.

Nano carbon containing low carbon magnesia carbon bricks are studied in the present work with a variation in the nano carbon content between 0-1.5 wt%. Total carbon content used for these bricks was around 5wt% compared to conventionally used bricks with 12-14wt% of carbon. The effect of reduction in carbon content and the use of nano carbon were studied by different characteristics of the bricks and the properties were compared against the conventional bricks prepared under similar manufacturing conditions.

Fused magnesia, nano carbon black and graphite were the starting raw materials with antioxidant metal oxide powder and resin and pitch as binder. The compositions were mixed and pressed and the shapes were then cured. Cured products were then characterized for various refractory properties.

Addition of nano carbon was found to improve the packing of the compositions and thus it improves the packing density, resulting an improvement in strength and decrease in the porosity. However at higher amount of nano carbon, the beneficial effect of packing is no more due to the excess presence of nano carbon, which increase the overall volume to the compositions and reduces the strength and increase porosity. Density was marginally improved initially but no great effect on physical and mechanical properties were found for the addition of nano carbon.

However the most beneficial effect was found for the HMOR and oxidation resistance. The main reason of such improvement is the higher reactivity of the nano carbon and resulting in a higher formation of carbide phases that improves the hot properties. Again for oxidation resistance, reduction in total carbon content and formation of carbide phases are the reasons for improvement. The present study showed that presence of 0.9wt% of nano carbon along with 3 wt% graphite results the best properties. Variation in graphite content at 0.9wt% of nano carbon also showed the same combination, that is 3 wt% graphite and 0.9wt% of nano carbon resulted in best properties. Another study on the variation in antioxidant quality

showed that use of 0.5 wt% of Al metal powder and 0.5 wt% of B₄C is the best combination of antioxidant.

Scope of future work:

The results so far obtained are highly encouraging and the main suggestions for the scope for future work are as follows.

- Details study of thermal conductivity of different low carbon MgO-C brick using nano carbon.
- Use of nano graphite in place of conventional graphite.
- Reduce the fixed carbon content upto 1wt%.
- Field trials to be carried out with the low carbon MgO-C bricks in steel ladle.
- Mixing of nano carbon along with other ingredients of MgO-C brick in the mixture machine was very difficult and cumbersome. So new technology to be developed to ease the incorporation of the nano carbon uniformly in MgO-C refractory system.

REFERENCES:

1. Annual book of ASTM standards, Refractories: Activated carbon, Advanced ceramics, 15.01, pp.19 (2003)
2. Kingery, W.D., Bowen, H.K., and Uhlmann, D.R., "Introduction to ceramics". John Wiley and sons, New York, (1976).
3. S.N. Laha, "Non recovery coke ovens "An overview and an innovative Indian refractories Experience" Vol.9, NO.1 February 2006 "IIM Metal News".
4. Tassot, P., Etinne, F., Wang, J., and Atkinson, P., "New concepts for steel ladle linings", Proc. UNITCER'07, Dresden, Germany, PP.462-465 (2007).
5. Inuzuka, T., "Technical development for steel making process", Nippon Steel technical report No:98, pp.63-69 (2008).
6. Exenberger, R., Moser, H., Niederhammer, K., Heiss, J., and Hoefer, W., "Improvement of the refractory lining in the Id-converter at Voestalpine Stahl GmbH LINZ, Australia," Proc. UNITCER'07, Dresden, Germany, pp.73-76 (2007).
7. Majumder, S., "Improvement in lining life", Advances in refractories for steel making, 2007, RDCIS, Ranchi (2007).
8. Gruber, D., Auer, T., and Harmuth, H., "Influence of an irreversible expansion of a teming ladle lining on its thermo-mechanical behaviour", 51st Intl. Colloq. on Refractories, Anchen, Germany, pp.73-75 (2008).
9. Barua, P., "Experiences in BOF's and steel ladles at SMS-II RSP", Advances in refractories for steel making, RDCIS, Ranchi (2007).
10. Figueiredo Jr, A., Bellandi, N., Vanola, A., and Zamboni, I., "Technological evolution of magnesia-carbon bricks for steel ladles in Argentina," Iron and steel technology, 1 pp.42-47 (2004).
11. Buchebner, G., Sampayo, L., Samm, V., Blondot, P., Peruzzi, S., and Boulanger, P., "ANKERSYN-A new generation of carbon-bonded magnesia carbon bricks", RHI Bulletin, pp.24-27 (2008).
12. Chatterjee, S., and Eswaran, R., "Continual improved performance MgO-C refractory for BOF", Proc. UNITCER'09, Salvador, Brazil, Article ID.136 (2009).
13. Tamura, S.-I., Ochiai, T., Takanga, S., Kanai, T.-A., and Nakamura, H., "Nano-tech. Refractories - 1: The development of nano structural matrix", Proc. UNITCER'03, Osaka, Japan, pp.517-520 (2003).
14. Takanga, S., Ochiai, T., Tamura, S., Kanai, T., and Nakamura, H., "nano-tech. Refractories -2: The application of the nano structural matrix to MgO-C bricks," Proc. UNITCER'03, OSAKA, Japan, pp.521-524 (2003).
15. Ochiai, T., "Development of refractories by applying nano technology", TARJ, 25, pp.4-11 (2001).
16. J.E.lee, I.kBae, Yang Moon Cho, Chang-Jung Um, "Development of low carbon MgO-C bricks for RH Degasser" pp.159 EUROGRESS, Aachen, Germany (2010).
17. S.Takanga, Y.fujiwara, M.Hatta, T.Ochiai and S.Tamura, "Development of MgO rimmed MgO-C Brick," pp.148-151 UNITCER (2005).

18. C.G.Aneziris,D.Borzov and M.Hampel, "Flexibility of MgO-C Refractories due to the bending tests at room temperature and after thermal shock treatment ," pp.261-264 UNITCER (2005).
19. A.Watanabe,H.Takahasi,T.Maqtzuki and M.Takahasi , "Some properties of Magnesita carbon Bricks containing mg and Al"pp.7-12 Tikabutsu (1985).
20. T.Matsumura, S.Uto,K.Hosokawa and M.Gegi, "properties of mahnesium carbon bricks containing Aluminium or Aluminium Alloys."pp.24-26Taikabustu (1988).
21. Hand book of refractories
22. G.D.Pickering ,J.D.Batchelor, "Carbon –MgO Reactions in BOF Refractories, pp.611-614,Vol.50,No.7,(1971).
23. Aneziris, C.G., Borzov, D., and Ulbricht, J., "Magnesia carbon bricks-a high-duty refractory material", Intr. Ceram Refract. Man., pp.22-27 (2003).
24. FigueiredoJr, A., Bellandi, N., Vanola, A., and Zamboni, I., "Technological evolution of magnesia carbon bricks for steel ladles in Argentina", Iron and Steel Technology, 1 pp.42-47 (2004).
25. Sune Jansson "A study on Molten Steel/Slag/Refractory Reactions during Ladle Steel Refining." ISRN KTH Stockholm (2005).
26. Blumenfeld, P., Peruzzi, S., Puillet, S., and de Lorgeril, J., "Recent improvents in Arcelor Steel Ladles", La Revue de Metallurgie CIT, 3, pp.233-239 (2005).
27. Tassot, P., Etienne, F., Wang, J., and Atkison, P., "New concepts for Steel Ladle linings", Proc. UNITCER'07, Dresden, Germny, pp.462-465 (2007).
28. Inuzuka, T., "Technical development of refractories for steel making process", Nippon steel technical report No:98, pp.63-69 (2008).
29. Barua, P., "Experiences in BOFs and steel ladles at SMS-II, RSP", Advances in refractories for steel making, RDCIS, Ranchi (2007).
30. Ewais, E.M.M., "Carbon based refractories", J. Ceram. Soc. Jpn., 112, pp.517-532 (2004).
31. Qeintela, MA., Santos, FD., Pessoa CA., Rodrigues, JA., and Pandolfelli, VC., "MgO-C refractories for steel ladles slag line", Refractories Applications and news, 11, pp.15-19 (2006).
32. Buchener, G., and Piker, S., "New high performance refractories for BOF vessels", Veitsch-RadexRundchau, 2, pp.3-14 (1996).
33. Ruh, E., "Refractories: Magnesita-Carbon Refractories, History, Development, Types and Applications", International Ceramic Monographs, 1, pp.772-793 (1994).
34. Hashemi, B., Nemati, Z.A., and Faghihi-Sani, M.A., "Effects of resin and graphite content on density and oxidation behavior of MgO-C refractory bricks", Ceram. Int., 32, pp.313-319 (2006).
35. Yamaguchi, A., "Control of oxidation-reduction in MgO-C refractories", Taikabutsu Overseas, 4, pp.32-36 (1984).
36. Missen, R.W. and Mims, C.A., "Introduction to chemical reaction engineering and kinetics", John Wiley and Sons Inc., New Yorky, pp.224 (1999).
37. Anan,K., "Wear of refractories in basic oxygen furnaces (BOF)", Taikabutsu Overseas, 21, pp.241-246 (2001).

38. Maekawa, A., Geji, M., Tanaka, M., Kitai, T., and Furukawa, K., "Influence of impurities in fused magnesia on the properties of MgO-C bricks", *Tarj*, 21, pp.74 (2001).
39. Tanaka, M., Maekawa, A., Hokii, T., Asano, K., and Ohtsuka, K., "Relationship between MgO aggregate purity and properties of MgO-C brick after firing in a reducing atmosphere", *Tarj*, 21 pp.215 (2001).
40. Minami, Y., Fuchimoto, H., Hokii, T., and Asano, K., "Effect of MgO purity on the corrosion resistance of MgO-C bricks against high temperature iron oxide slag", *TARJ*, 21 pp.212 (2001).
41. Staron, J. and Palco, S., "Production technology of magnesia clinker", *Am.Ceram.Soc.Bull.*, 72, pp.83-87 (1993).
42. Yoshida, A., "On the present status of sea water magnesia manufacturing" , *TARJ*, 25, pp.89-99 (2005).
43. Nameishi, N., Ishibashi, T., Matsumura, T., Hosokawa, K., and Tsuchinai, A., *Taikabutsu*, 32 pp.583-587 (1980).
44. Ishii, H., Tsuchiya, I., Oguchi, Y., Kawamaki, T., and Takahashi, H., "Bhaviour of impurities in magnesia carbon brick at high temperatures", *Taikabutsu Overseas*, 10, pp.3-8 (1999).
45. Matsuo, A., Miyagawa, S., Ogasawara, K., Yokoi, M., Uchimura, R., and Kumagai, M., *Taikabutsu*, 36, pp.644-647 (1984).
46. Matsui, K., and Kawano, F., "Effect of impurities in magnesia on reaction between magnesia clinker and carbon", *Taikabutsu Overseas*, 14, pp.3-12 (1994).
47. Kuffa, T., Sucik, G., and Hrsak, D., "The influence of carbon materials on the properties of MgO refractories", *Materials and Technology*, 39, pp.211-213 (2005).
48. Tanaka, S., Okajima, S., Sugimoto, T., and Fujio, M., *Taikabutsu*, 35, pp.643-646 (1983).
49. Rita, K., John, S., and Veena, S., "Role of ash impurities in the depletion of carbon from alumina graphite mixtures in two liquid iron", *ISIJ International*, 47, pp.282-288 (2007).
50. Sakaguchi, M., Ishii, H., Aratani, K., and Oguchi, Y., "Effect of graphite particle size on properties of MgO-C bricks", *Taikabutsu*, 44, pp.700-707 (1992).
51. Tamka, P and Baldo J.B, "A new friendly resin with coupled anti-oxidants protectors for carbon containing refractories, UNITCER'07, pp.30 (2007).
52. Nishimura, D., " Technical trends of phenolics for Japanese refractories", *Taikabutsu Overseas*, 15, pp.10-14 (1995).
53. S. Zhang, N.J. Marriott, W.E. Lee, Thermochemistry and microstructures of MgO–C refractories containing various antioxidants, *J. Eur. Ceram.Soc.* 21 (2001) pp.1037–1047.
54. S. Uchida, K. Niihara, K. Ichikawa, High-temperature properties of unburned MgO–C bricks containing Al and Si powders, *J. Am. Ceram.Soc.* 81 (1998) pp.2910–2916.
55. C. Baudin, C. Alvarez, R.E. Moore, Influence of chemical reactions in magnesia–graphite refractories. I. Effects on texture and high-temperature mechanical properties, *J. Am. Ceram. Soc.* 82 (1999) pp.3529–3538.

56. K. Ichikawa, H. Nishio, O. Nomura, Y. Hoshiyama, Suppression effects of aluminum on oxidation of MgO–C bricks, *Taikabutsu Overseas* 15 (1995) pp.21–24
57. C. Taffin, J. Poirier, The behaviour of metal additives in MgO–C and Al₂O₃–C refractories, *Interceram* 43 (1994) pp.354–358.
58. A.S. Gokce et al. *Ceramics International* 34 (2008) pp.323–330
59. TakafumiImaeda “Effect of boron containing additives on magnesia carbon bricks”, *Taikabutsu*, Vol.24, pp.216.
60. Harada, T., Matsuura, O., Uchida, M., and Takahashi, H., “Comparison of the characteristics of MgO-C bricks formed by different pressing methods”, *TARJ*, 21, pp.172-176(2001).
61. Gleiter,H., “Nano crystalline materials :basic concepts and microstructure”,*Acta Mater.*,48 (2000),pp.1-29;
62. Tionj,S., and Chen ,H., “Nano crystalline materials and coatings”,*Mater.Sic.Eng.Res.*,45,pp.1-88(2004)
63. Chen ,M.,Lu,C., and Yu, J., “Improvement of performance of MgO-CaO refractories by addition of nano sized ZrO₂”,*J.Euro .Ceram .Soc.*,27,pp.4633-4638 (2007).
64. Azhari, A., Golestani-Fard, F., and Sarpoolaky,H., “Effect of nano iron oxide as an additive ofn phase and microstructural evolution of Mag-Chrome refractory matrix”,*J.Euro.Ceram.Soc.*,29,pp.2679-2684 (2009).
65. Satpathy, S., “Influence of nano Fe₂O₃ on the microstructure and property development of silica brick”,*M.Tech thesis ,NIT –Rourkela* (2008).
66. C. Tani, H. Sugimoto, O. Nomura, N. Kurashina and Y. Hoshiyama, *Shinagawa Technical Report* Vol.38 (1995) pp.25-32.
67. K. Moriwaki, Y. Hoshiyama, Q. Nomura and K. Ichikawit, *Taikabutsu* 49[11]600 (1997).
68. Y. Hosiya, K. Moriwaki and O. Nomura, *Taikabutsu* 50[8]426(1998).
69. Ochiai T. The Development of Refractories by Applying Nano-technology. *Taikabustu*, 2004, 56(4): pp.152-159.
70. Yang Xuejun, QiuZheming and Hu Liangquan. The Influence of Nanometer Carbon Black on the Mechanical Properties of Phenolic Resin. *Processing of aircraft materials*, 2003, 33(4)pp. 34-38.
71. Li Xianhui, Wu Chifei. The optimization of characterization and preparation on nanometer carbon blacks. *Processing technology of nanometer materials*, 2005, 2(5): pp.47-49.
72. SHAW K., *Refractories and Their Uses*, Applied Science Publishers Ltd., London, 1972.
73. CHANDLER H. W., *Thermal Shock of Refractories*, Proc. Tehran Int. Conf. of Refractories, 2004, 28–39.
74. American Society of Testing and Materials Standards, Sect. 15, Vol. 15.01, 1990.
75. British Standard Testing of Engineering Ceramics, BS 7134, Section 1.2, 1989.